



## OPEN ACCESS

## EDITED BY

Pin-Xian Xu,  
Icahn School of Medicine at Mount Sinai,  
United States

## REVIEWED BY

Alberto Rosello-Diez,  
University of Cambridge, United Kingdom  
Matthew Anderson,  
National Cancer Institute at Frederick (NIH),  
United States

## \*CORRESPONDENCE

Debora Sinner,  
✉ debora.sinner@cchmc.org

## †PRESENT ADDRESS

Megha Mohanakrishnan,  
College of Medicine, University of Cincinnati,  
Cincinnati, OH, United States  
Kaulini Burra,  
Nationwide Children's Hospital, Columbus,  
OH, United States  
Yixin Wu,  
Division of Biology and Biomedical Sciences,  
Washington University in St. Louis, St. Louis,  
MO, United States

RECEIVED 06 November 2024

ACCEPTED 04 March 2025

PUBLISHED 09 April 2025

## CITATION

Bottasso-Arias N, Mohanakrishnan M,  
Trovillion S, Burra K, Russell NX, Wu Y, Xu Y  
and Sinner D (2025) Wnt5a and Notum  
influence the temporal dynamics of  
cartilaginous mesenchymal condensations in  
developing trachea.  
*Front. Cell Dev. Biol.* 13:1523833.  
doi: 10.3389/fcell.2025.1523833

## COPYRIGHT

© 2025 Bottasso-Arias, Mohanakrishnan,  
Trovillion, Burra, Russell, Wu, Xu and Sinner.  
This is an open-access article distributed  
under the terms of the [Creative Commons  
Attribution License \(CC BY\)](https://creativecommons.org/licenses/by/4.0/). The use,  
distribution or reproduction in other forums is  
permitted, provided the original author(s) and  
the copyright owner(s) are credited and that  
the original publication in this journal is cited,  
in accordance with accepted academic  
practice. No use, distribution or reproduction  
is permitted which does not comply with  
these terms.

# Wnt5a and Notum influence the temporal dynamics of cartilaginous mesenchymal condensations in developing trachea

Natalia Bottasso-Arias <sup>1†</sup>, Megha Mohanakrishnan <sup>2</sup>,  
Sarah Trovillion <sup>1</sup>, Kaulini Burra <sup>1†</sup>, Nicholas X. Russell <sup>2</sup>,  
Yixin Wu <sup>1†</sup>, Yan Xu <sup>1,3</sup> and Debora Sinner <sup>1,3\*</sup>

<sup>1</sup>Neonatology and Pulmonary Biology, Perinatal Institute, Cincinnati Children's Hospital Medical Center, Cincinnati, OH, United States, <sup>2</sup>Neonatology and Pulmonary Biology, Perinatal Institute, Cincinnati Children's Hospital Medical Center and University of Cincinnati Honors Program, Cincinnati, OH, United States, <sup>3</sup>University of Cincinnati, College of Medicine, Cincinnati, OH, United States

**Introduction:** The trachea is essential for proper airflow to the lungs for gas exchange. Frequent congenital tracheal malformations affect the cartilage, causing the collapse of the central airway during the respiratory cycle. We have shown that Notum, a Wnt ligand de-acylase that attenuates the canonical branch of the Wnt signaling pathway, is necessary for cartilaginous mesenchymal condensations. In Notum deficient tracheas, chondrogenesis is delayed, and the tracheal lumen is narrowed. It is unknown if Notum attenuates non-canonical Wnt signaling. We observed premature tracheal chondrogenesis after mesenchymal deletion of the non-canonical Wnt5a ligand. We hypothesize that Notum and Wnt5a are required to mediate the timely formation of mesenchymal condensations, giving rise to the tracheal cartilage.

**Methods/Results:** *Ex vivo* culture of tracheal tissue shows that chemical inhibition of the Wnt non-canonical pathway promotes earlier condensations, while Notum inhibition presents delayed condensations. Furthermore, non-canonical Wnt induction prevents the formation of cartilaginous mesenchymal condensations. On the other hand, cell-cell interactions among chondroblasts increase in the absence of mesenchymal Wnt5a. By performing an unbiased analysis of the gene expression in Wnt5a and Notum deficient tracheas, we detect that by E11.5, mRNA of genes essential for chondrogenesis and extracellular matrix formation are upregulated in Wnt5a mutants. The expression profile supports the premature and delayed chondrogenesis observed in Wnt5a and Notum deficient tracheas, respectively.

**Conclusion:** We conclude that Notum and Wnt5a are necessary for proper tracheal cartilage patterning by coordinating timely chondrogenesis. Thus, these studies shed light on molecular mechanisms underlying congenital anomalies of the trachea.

## KEYWORDS

Wnt, Notum, cartilage, morphogenesis, patterning, respiratory tract

## Introduction

Patterning the developing respiratory tract requires precise interactions between the endoderm-derived epithelium and the surrounding mesenchyme (Caldeira et al., 2021; Nasr et al., 2020; Shannon and Hyatt, 2004). This feedback is essential to determine the branching pattern of the developing lung (Zhang et al., 2022), pulmonary epithelial cell differentiation (Brownfield et al., 2022), as well as cell differentiation of the mesenchyme and epithelium of the central airways of the respiratory tract (Bottasso-Arias et al., 2022; Zhou et al., 2022). Our previous studies have identified Notum as a target of epithelial Wls-mediated signaling that influences mesenchymal condensation and cartilaginous ring morphology. Furthermore, Notum is an essential component of a negative feedback loop attenuating Wnt/ $\beta$ -catenin signaling in developing mesenchyme (Gerhardt et al., 2018).

Wnt5a, a Wnt ligand triggering non-canonical response in developing respiratory tract, plays roles in epithelial cell differentiation and alveolarization, partially by inhibiting Wnt/ $\beta$ -catenin signaling via mechanisms dependent on Ror1/2 (Baarsma et al., 2013; Li et al., 2020). Aberrant expression of Wnt5a is also associated with cancerous lung disease, pulmonary fibrosis, bronchopulmonary dysplasia (BPD), and hyperoxia injury (Sucre et al., 2020). Non-canonical signaling exerts a critical role in the convergent extension movements of cells via planar cell polarity (PCP), supporting the elongation of different structures during development (Tada and Heisenberg, 2012), the position and branching pattern in developing lung (Zhang et al., 2022), tracheal length (Kishimoto et al., 2018), and the orientation and assembly of the epithelium and smooth muscle cells of the trachealis muscle (Kishimoto et al., 2018; Russell et al., 2023). Notably, in developing trachea, we detected a precise pattern of expression wherein Notum expression is positioned between epithelial Wnt7b (a ligand inducing Wnt/ $\beta$ -catenin (Wang et al., 2005)) and mesenchymal-produced non-canonical Wnt5a (Figure 1A). However, whether Notum can modulate non-canonical Wnt signaling and its effect on morphogenesis and disease outcome remains unclear.

Previous studies have shown that anomalous cartilage patterning leads to congenital malformations such as tracheomalacia, a genetic structural abnormality of the trachea with weak cartilage lining, and tracheal stenosis, with both impairing breathing. We identified compound heterozygous single nucleotide variant (SNV) in ROR2 in patients diagnosed with complete tracheal ring deformity (CTRD), a condition characterized by tracheal stenosis (Sinner et al., 2019). ROR2 encodes the receptor of WNT5A supporting a role for the ligand Wnt5a via ROR2 mediated signaling in the patterning of the central airways of the respiratory tract in humans.

Chondrogenesis leading to mature cartilage is a tightly regulated process encompassing morphogenetic events and phenotypic changes (Goldring et al., 2006). The first step in chondrogenesis is cell condensation and the formation of condensed cell aggregates. The process of mesenchymal condensation primarily involves an increase in local cell density, mediated by local cell movements without altered proliferation (Klumpers et al., 2014). These local cell rearrangements are mediated by passive extracellular matrix ECM-driven movements and by dragging and pushing by neighboring cells (Oster et al., 1985; Cui et al., 2005). Studies by Barna and Niswander (Barna and Niswander, 2007) demonstrated in an *in*

*vitro* model with single cell imaging resolution, that the process of mesenchymal condensation is very dynamic requiring sorting, migration and cell shape changes partially mediated by Sox9 and Bmp4. At this early stage in mesenchymal condensation formation, the major components of the ECM are hyaluronic acid and fibronectin (FN) (Knudson and Toole, 1985; Kulyk et al., 1989). Simultaneously, cell-cell contacts mediated through N-cadherin and neural cell adhesion molecule (N-CAM), are increased to facilitate cell-cell communication likely triggering the onset of chondrogenic differentiation (Widelitz et al., 1993). This model agrees with the notion that a high cell density is required for chondrogenesis (Mauck et al., 2002). Supporting this concept, studies on tooth development demonstrated that cell compaction causes the activation of a genetic cascade necessary for specific cell induction (Mammoto et al., 2011). While cellular events driving the cell condensation have been unveiled, less is known about how genetic cues are integrated and transduced into forces mediating cell compaction.

In the present work, we sought to investigate the role of Notum influencing the Wnt5a-mediated signaling in tracheal mesenchymal condensations that give rise to the tracheal rings. We hypothesize that Notum represses Wnt5a-mediated non-canonical Wnt signaling, which is required for tracheal mesenchyme patterning and cartilage formation. We determined that Wnt5a, similarly to Notum, is necessary for the timely condensation of chondroblasts, and its ablation causes precocious condensation affecting cartilaginous ring morphology and number. *In vivo*, Notum fine-tunes the Wnt canonical and non-canonical levels in developing tracheal mesenchyme to promote the formation and patterning of tracheal cartilage.

## Material and methods

### Mouse breeding and genotyping

Animals were housed in a pathogen-free environment and handled according to the protocols approved by CCHMC Institutional Animal Care and Use Committee (Cincinnati, OH, United States). Generation of a Notum loss of function allele, Notum<sup>150/150</sup> was previously described (Gerhardt et al., 2018). Adult Notum mice were kept in heterozygosis. Wnt5a<sup>fl/fl</sup> (Jackson lab # 026626) were mated with Dermo1<sup>Cre/wt</sup> (Jackson lab# 008712) to generate Dermo1<sup>Cre/wt</sup>; Wnt5a<sup>fl/wt</sup> mice and rebred to Wnt5a<sup>fl/fl</sup> generating embryos of genotype Dermo1Cre; Wnt5a<sup>fl/fl</sup> mice (Ryu et al., 2013). Notum<sup>300/150</sup> mice were bred with Wnt5a<sup>fl/fl</sup> (Jackson lab # 026626) mice to generate Notum<sup>300/150</sup> Wnt5a<sup>fl/wt</sup>, and the resulting mouse rebred to Wnt5a<sup>fl/fl</sup> to generate Notum<sup>300/150</sup> Wnt5a<sup>fl/fl</sup>. Notum<sup>300/150</sup> mice were bred with Dermo1<sup>cre/wt-</sup> (Jackson lab# 008712) to generate Notum<sup>300/150</sup> Dermo1<sup>cre/wt-</sup>. The Notum<sup>300/150</sup> Dermo1<sup>cre/wt-</sup> were then crossed with a Notum<sup>300/150</sup> Wnt5a<sup>fl/fl</sup> to produce Notum<sup>150/150</sup> Wnt5a<sup>fl/wt-</sup> Dermo1<sup>cre/wt-</sup> embryos. Sox9KieGFP mice were previously described (Chan et al., 2011) (Jackson laboratories # 030137). Genotypes of transgenic mice were determined by PCR using genomic DNA isolated from mouse-tails or embryonic tissue.  $\gamma$ SMA mouse was previously described (Bottasso-Arias et al., 2022; Russell et al., 2023). Primers utilized for genotyping are provided as (Supplementary Table S1).

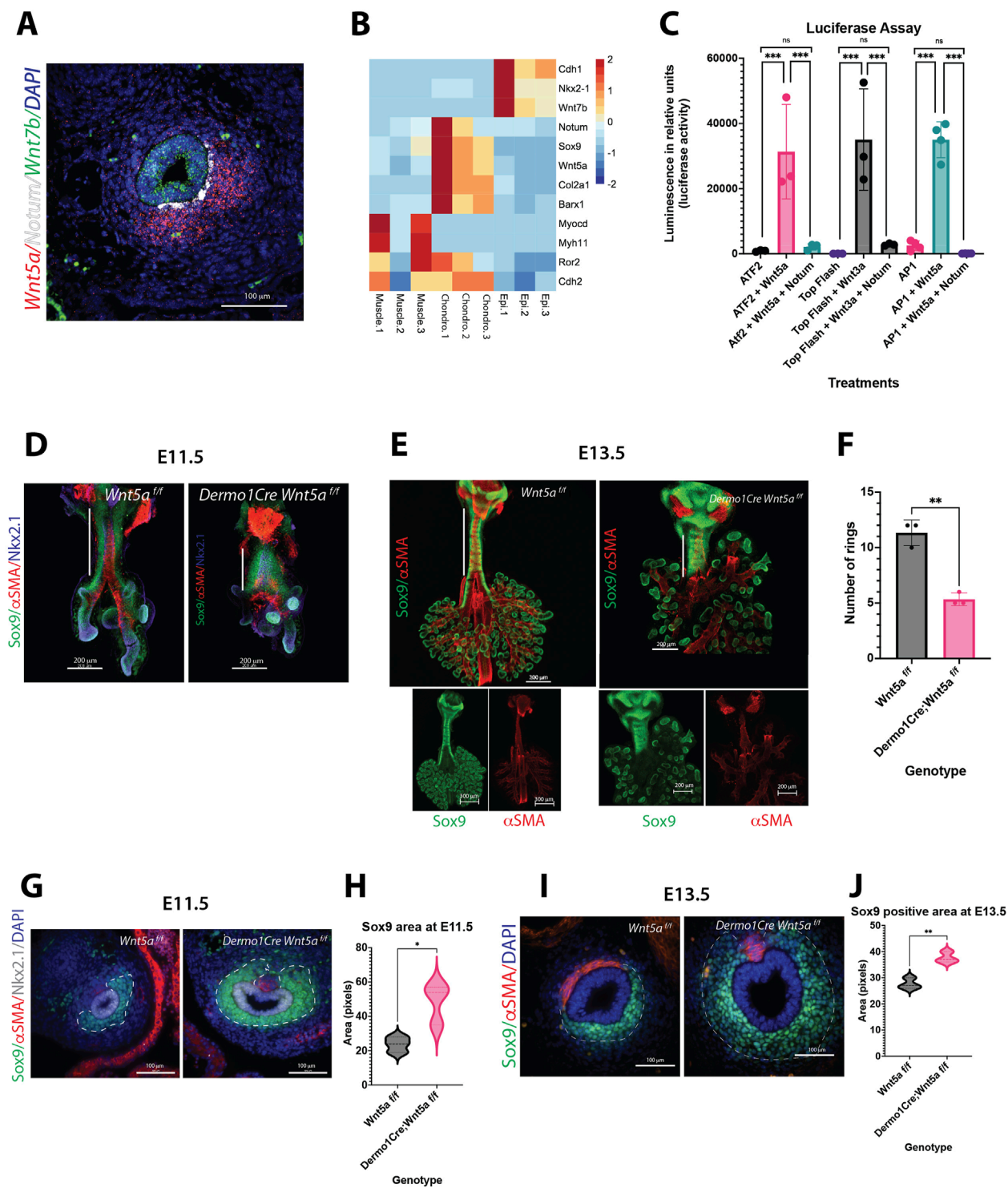


FIGURE 1

Wnt5a controls cartilage development, while Notum abrogates Wnt5a activity. (A) RNA *in situ* hybridization of E13.5 cross section depicting the localization pattern of Wnt non-canonical ligand *Wnt5a* (red) in the ventrolateral region of the trachea mesenchyme, and canonical ligand *Wnt7b* (green) expressed in the epithelium of the trachea. *Notum* (white) is located in the mesenchymal, subepithelial region in between *Wnt5a* and *Wnt7b* areas of expression. DAPI (blue) was used to stain the nuclei. 40x image. (B) Heatmap of RNAseq from cell sorted tracheal cells isolated at E13.5. Epi. antibody stained EpCAM (+) cells, Muscle. endogenous SMA-eGFP (+) cells, Chondro. EpCAM (-), SMA-eGFP (-) double negative cells. *Notum* and *Wnt5a* are expressed in chondroblast cells, identified by the expression of chondrogenic genes: *Col2a1* and *Sox9*. Otherwise absent in muscle and epithelial cells. (C) Luciferase assay performed on NIH3T3 cells transfected with ATF2, TOP Flash or AP1 reporter constructs. Co-transfection of *Wnt5a* expression plasmid increases the luciferase activity by the TOP Flash construct. In all cases, when *Notum* expression plasmid is also added, this luciferase induction is abrogated. In this *in vitro* assay, *Notum* can dampen the activities of canonical (*Wnt3a*) and non-canonical (*Wnt5a*) ligands. n = 3 for each treatment group. \*\*\*p < 0.001, ns non-significant statistical differences. One-way ANOVA (D-E) Wholemount immunofluorescence (IF) of dissections of larynx-trachea-lungs at (D)

(Continued)

## FIGURE 1 (Continued)

E11.5 and (E) E13.5 of control (*Wnt5a<sup>fl/fl</sup>*) and *Wnt5a* mutants (*Dermo1cre; Wnt5a<sup>fl/fl</sup>*). Sox9 (green) is expressed in chondroblasts and epithelial cells of the distal lung.  $\alpha$ SMA (red) is localized in muscle cells of the dorsal trachea and bronchi. This expression pattern is maintained in *Wnt5a* mutants compared to controls, but the trachea is shorter in length (white vertical full line) with defects in lung lobation noticeable by E13.5. At E11.5, there is no evidence of ring formation as noticed by the Sox9 (+) continuum observed in the trachea mesenchyme. At E13.5, Sox9 (+) cells in the trachea appear more defined in rings for *Wnt5a* mutants than controls. Dorsal trachea muscle cells ( $\alpha$ SMA (+)) show defects in orientation, particularly towards the proximal region, closer to the larynx. Scale bars: 200  $\mu$ m for E11.5 samples, 300  $\mu$ m for the E13.5 control image, and 200  $\mu$ m for the E13.5 *Wnt5a* mutant image. Single channels are shown for whole mounts at E13.5 (F) Reduction in the tracheal ring number by E14.5 in mutants vs. controls.  $n = 3$  for each genotype.  $**p < 0.01$  (G) IF of cross sections of control and *Wnt5a* mutant at E11.5. Chondroblasts are Sox9 (+) (green), muscle cells are  $\alpha$ SMA (+) (red), and respiratory epithelial cells are Nkx2.1 (+) (grey). In *wnt5a* mutants Sox9 (+) area is larger than the controls. (H) Sox9 staining intensity quantification of (G) within the area delimited by a dashed white line.  $n = 3$   $*p < 0.05$  (I) IF of cross sections of E13.5 embryos. Sox9 (+) (green) area (delimited by a dashed white line) is larger in *Wnt5a* mutants compared to controls. Sox9 expression also extends dorsally. Muscle cells ( $\alpha$ SMA (+), red) are organized differently in *Wnt5a* mutants vs. controls. 40x images. (J) Sox9 staining intensity quantification of (I) within the area delimited by a dashed white line.  $n = 3$   $**p < 0.01$ .

## DNA constructs

Plasmid utilized for transfection were pGL2 Top Flash, (Sinner and Hyatt, 2004), pcDNA3 Full Length Notum, (GenScript), pGL2ATF2 (a gift from Dr. Niehrs) (Ohkawara and Niehrs, 2011), pGL3AP1 (Addgene), pcDNA6 active*Wnt5a*, and pcDNA6 active*Wnt3a* (Addgene).

## Transfections and luciferase assay

NIH3T3 cells were cultured in 48 well plate, at 37°C and 5% CO<sub>2</sub>. Cells at 60%–70% confluency were transfected with a total of 50 ng of plasmidic DNA using Fugene (Promega) according to manufacturer's instructions. These reporters were co-transfected with *Wnt3a*, *Wnt5a* and/or Notum expression plasmids (Gerhardt et al., 2018). Cells were harvested 24 h post transfection, washed with PBS, and lysed using a passive lysis buffer reagent (Promega). Luciferase activity was determined over 10 s integration time using a luminometer (Promega).

## Dissociation and FACS of embryonic trachea

Cell dissociation was performed following a previously published protocol (Bottasso-Arias et al., 2022). Per each sample, five E13.5  $\gamma$ SMA<sup>eGFP</sup> tracheas/litter were pooled together and dissected in cold PBS and dissociated to single cells using TrypLE Express (phenol-red free, Thermo, 12604013) at 37°C for 10 min, followed by trituration for 30 s at RT. Cells were washed twice with FACS buffer (1 mM EDTA, 2% FBS, 25 mM HEPES in phenol-red free HBSS). To identify epithelial cells, cells were stained with APC anti-mouse CD326/EpCAM (Invitrogen, ref 17-5791-82, used at 1:50) at 4°C for 30 min followed by two washes with FACS buffer. Cells were resuspended in FACS buffer and passed through a 35  $\mu$ m cell strainer. To stain dead cells, Sytox Blue nucleic acid stain (Thermo, S11348, used at 1  $\mu$ M) was added to the cell suspension. Cells were sorted using a BD FACS Aria I and II. Single live “chondroblast enriched cell population” was collected after size selection and gating for Sytox-negative, EpCAM-negative, and eGFP negative cells. Cells were sorted directly into RNA lysis buffer (Zymo Research Quick RNA Micro kit, S1050) for isolation of RNA. Cell isolation strategy was confirmed by qRT-PCR (Supplementary Figure S1) and

as previously shown (Bottasso-Arias et al., 2022; Russell et al., 2023). Data is shown for three independent samples.

## Transcriptomic analyses

RNA-sequencing data were generated and compared from E11.5 *Dermo1Cre; Wnt5a<sup>fl/fl</sup>* tracheas vs. E11.5 *Wnt5a<sup>fl/fl</sup>* tracheas and E13.5 *Notum<sup>150/150</sup>* vs. E13.5 *Notum<sup>300/300</sup>* chondroblasts (GEO repository under GSE260707). Differentially expressed genes were identified using Deseq2 (E11.5 *Wnt5a* tracheas  $N = 5$  Controls,  $N = 4$  Mutants; *Notum* E13.5 sorted chondroblasts  $N = 3$  controls,  $N = 4$  mutants) (Anders and Huber, 2010; Lawrence et al., 2013). Fragments Per Kilobase of transcript per million mapped reads (FPKM) values were calculated using Cufflinks (Trapnell et al., 2010). Differentially expressed genes were identified with the cutoff of a p-value <0.05, FC > 1.5 and FPKM >1 in over half of the replicates in at least one condition. The same approach was utilized for gene expression analysis of E13.5 control chondroblast, epithelium and smooth muscle cells isolated by FACS. (GEO repository GSE241175). Heatmaps were generated using normalized counts generated by DESeq2 and pheatmap or from RNA-seq fold changes. Functional enrichment was performed using Topfun and hits relevant to this project were visualized in a -log<sub>10</sub> (pvalue) bubble chart. System models were created using IPA's Path Designer.

## Whole mount staining

Tracheal lung tissues isolated at E11.5–E14.5 were subject to whole mount immunofluorescence as previously described (Sinner et al., 2019). Embryonic tissue was fixed in 4% PFA overnight and then stored in 100% Methanol (MeOH) at -20°C. For staining, wholemounts were permeabilized in Dent's Bleach (4:1:1 MeOH: DMSO: 30% H<sub>2</sub>O<sub>2</sub>) for 2 h, then taken from 100% MeOH to 100% PBS through a series of washes. Following washes, wholemounts were blocked in a 2% BSA (w/v) blocking solution for 2 h and then incubated, overnight, at 4°C in primary antibody diluted accordingly in the blocking solution. After five 1-h washes in PBS, wholemounts were incubated with a secondary antibody at a dilution of 1:500 overnight at 4°C. Samples were then washed three times in 1X PBS, transferred to 100% methanol, through a series

of washes in dilutions of methanol, and cleared in benzyl-alcohol benzyl-benzoate (Murray's Clear). Images of wholemounts were obtained using confocal microscopy (Nikon A1R). Imaris imaging software was used to convert z-stack image slices obtained using confocal microscopy to 3D renderings of wholemount samples.

## Immunofluorescence staining and quantification

Embryonic tissue was fixed in 4% PFA overnight and embedded in paraffin or OCT to generate 7  $\mu\text{m}$  sections. For general immunofluorescence staining, antigen retrieval was performed using 10 mM Citrate buffer, pH6. Slides were blocked for 2 h in 1XTBS with 10% Normal Donkey serum and 1% BSA, followed by overnight incubation at 4°C in the primary antibody, diluted accordingly in blocking solution. Slides were washed in 1X TBS-Tween20 and incubated in secondary antibody at 1:200, in blocking solution, at room temperature for 1 hour, washed in 1X TBS-Tween20, and cover-slipped using Vecta shield mounting media with or without DAPI. Fluorescent staining was visualized and photographed using automated fluorescence microscopes (Nikon). For cross sections in [Figure 1](#), the area of Sox9 positive cells was determined using ImageJ. For cross sections in [Figure 4](#), the intensity of the N-cadherin stainings was quantified and normalized to the Sox9 + area using NIS elements. Antibodies utilized in this manuscript have been previously validated by our laboratory and other investigators. Source, references, and dilution of primary and secondary antibodies used have been provided as Supplementary material ([Supplementary Table S2](#)).

## Embryonic tracheal-lung culture

Sox9KI (Sox9-GFP) Embryonic tracheas were harvested at E12.5 and cultured in air-liquid interphase for 42 h as described ([Hyatt et al., 2002](#)). Images were obtained at frequent intervals and timelapse videos were recorded overnight between 24 and 42 h employing an EVOS M7000 microscope ([Supplementary Videos S1–S4](#)). Samples were treated with vehicle (DMSO), ABC99 (25  $\mu\text{M}$  Sigma SML2410), KN93 (5  $\mu\text{M}$  Millipore Sigma 422,708), JNK inhibitor II (8  $\mu\text{M}$  Millipore Sigma 420,119) or XAV939 (10  $\mu\text{M}$ , inhibitor of tankyrase I/II Biotechnie Tocris 3748). Wnt5a conditioned media was obtained from L cells (ATCC cat no. CRL-2647CRL-2814) and was diluted 50% with growth media (DMEM 5% FBS) for the experiment.

## Tracheal mesenchymal cell isolation and culture

Primary cells were isolated as previously described ([Bottasso-Arias et al., 2022](#); [Gerhardt et al., 2018](#)). Briefly, E13.5 tracheas of at least five embryos of the same genotype were isolated, washed in 1X PBS, dissociated in TrypLE express (Gibco) and incubated for 10 min at 37°C. After incubation, tissue was pipetted until cell suspension formed. Cells were seeded in flasks containing MEF tissue culture media composed of DMEM

(ATCC 30-2002), 1% penicillin/streptomycin (Gibco 15140122), 2% antibiotic/antimycotic (Gibco 15240062), and 20% non-heat inactivated FBS (R&D S11150). Only mesenchymal cells were attached, as we confirmed expression of Sox9, Col2a1 and Myh11 but no expression of Nkx2.1 was detected ([Bottasso-Arias et al., 2022](#)).

## Wound-healing assay

Procedure was performed according to the manufacturer's instructions using Culture-Inserts 2 Well (Ibidi) on a 24-well plate. A suspension of  $8 \times 10^5$  trachea MEF cells per mL isolated from control and *Wnt5a* and *Notum* knockout cells were plated on each side of the insert. A day after seeding, the inserts were removed, and a live cell nuclear dye (NucBlue ReadyProbe R10477, Invitrogen) was added to the cell media. The 24-well plate was then placed in an Evos M7000 microscope with an incubator (Thermo Fisher) (37°C and 5% CO<sub>2</sub>) overnight and timelapse images were taken with 20-min time intervals between images for brightfield and DAPI channels. The total incubation time was 24 h. ImageJ was used to measure the wound area from the brightfield images at various time points.

## Directional migration

Haptotaxis assay was performed using the CytoSelect 24-well kit (8  $\mu\text{m}$ , fibronectin coated, colorimetric format) according to the manufacturer's instructions (CBA-100-FN, Cell Biolabs Inc.). Briefly, 300  $\mu\text{L}$  of a suspension of  $1.0 \times 10^6$  cells/mL was seeded inside the insert for each cell type (Notum control and mutant cells, Wnt5a control and mutant cells). Cells were allowed to migrate to the bottom of the insert coated with fibronectin for 24 h. Afterwards, the remainder of the cells was removed from the inside of the insert and the cells that migrated to the bottom of the insert coated with fibronectin were stained with the dye. After washes and drying the inserts, the dye was solubilized and 100  $\mu\text{L}$  were transferred to a 96-well plate to measure absorbance at 560 nm in a plate reader (Spectra MR Dynex Technologies). N = 5 for each genotype.

## Cell adhesion

Cell adhesion assays were performed using micromasses plated with the different cell types (Notum control and Notum mutant, Wnt5a control and Wnt5a mutant). 50,000 cells per micromass were seeded in a 24-well plate. After allowing the micromasses to adhere for 2 h, they were washed with PBS and fixed with 100% methanol. The micromasses were then stained with 0.1% Crystal Violet diluted in distilled water. The staining was removed, and the wells were washed with distilled water. A lysis-resuspension solution consisting of 10% methanol and 5% glacial acetic acid was added to each well, and cells were resuspended. 60  $\mu\text{L}$  of the cells were transferred to a 96-well plate and the absorbance was read between 570–585 nm. A comparison between the absorbance of control and mutant cells was used relatively to determine cell adhesion.

## In-situ hybridization and quantification

The procedure was performed according to a protocol developed by Advanced Cell Diagnostics (ACD) (Wang et al., 2012). *In situ* probes were designed by ACD. Slides were baked and deparaffinized. *In situ* probes were added to the slides and hybridization was performed for 2 h at 40°C, followed by several rounds of amplification steps. For fluorescence detection, opal dyes were utilized to detect the localization of the transcripts. After mounting with permanent mounting media (ProLong Gold, Thermo), slides were photographed using a wide field Nikon fluorescent microscope. Quantification was performed using NIS elements. Regions of Interest (ROI) were selected and mean intensity was obtained for individual channels.

## Statistics

Quantitative data were presented as mean  $\pm$  standard error. For animal experiments, a minimum of three different litters for each genotype were studied. Experiments were repeated at least twice with a minimum of three biological replicates for each group. Statistical analysis was performed using Graph Pad Prism ver.10 for MacOS. Statistically significant differences were determined by paired T-test, or one-way or two-way ANOVA repeated measures followed by *post hoc* pairwise multiple comparison procedures (Dunnett or Holm-Sidak test). Significance was set at  $P < 0.05$ .

## Results

### Notum attenuates non-canonical Wnt signaling, and is needed for proper cartilage development

Published studies have demonstrated that Notum and Wnt5a are involved in forming and patterning the tracheal cartilaginous rings. At E13.5, Notum is localized in the ventral subepithelial mesenchyme of the trachea, and Wnt5a is localized in the ventral mesenchyme of the trachea, just outside the localization of Notum (Figure 1A). In both cases, Wnt5a and Notum were found to be in the region where tracheal cartilage forms and wherein Col2a1 and Sox9 are expressed, as determined by RNAseq from sorted tracheal cells isolated at E13.5 from gSMAe-GFP mouse embryos (Russell et al., 2023). In this experiment, epithelial cells (Epi) were identified by antibody staining using EpCAM (+), Muscle cells were identified by endogenous gSMA-eGFP (+) signal, The chondrocyte enriched population was defined as EpCAM (-), SMA-eGFP (-) double negative cells expressing chondrogenic genes: Col2a1 and Sox9 absent in muscle and epithelial cells. (Figure 1B; Supplementary Figure S1). Notably, Wnt7b (a ligand inducing Wnt/ $\beta$ -catenin dependent signal) is observed in the epithelium overlapping with Nkx2.1 and Cdh1 (Figures 1A, B). Barx1, a gene involved in inter-zone formation between cartilages of the limb (Yadav et al., 2023), is detected in cells contributing to chondroblasts and excluded from myoblasts and epithelial cells (Figure 1B). The complementary and distinct localization of Wnt7b, Notum, and Wnt5a in developing trachea supports a

role for Notum in regulating the levels and the types of activity triggered by Wnt7b and Wnt5a. As previously shown, Notum can attenuate the activation of Top Flash by the canonical ligand Wnt3a (Gerhardt et al., 2018; Kakugawa et al., 2015). Similarly, Notum reduces Wnt5a-induced activation of ATF2 (Ohkawara and Niehrs, 2011; Wallkamm et al., 2014) and AP1 promoters (Figure 1C) (Nishita et al., 2010). These two transcription factors are part of the Wnt non-canonical/Planar Cell Polarity pathway and are downstream of JNK (Voloshanenko et al., 2018). These results suggest that Notum can deactivate ligands from canonical and non-canonical Wnt signaling.

To better understand Wnt5a's putative role in cartilaginous ring formation, we deleted Wnt5a from the splanchnic mesoderm using *Dermo1Cre*. Although our previous studies have shown expression of Wnt5a in tracheal epithelium at E11.5, its expression becomes strongly localized to the mesenchyme by E13.5 ((Snowball et al., 2015a). Studies published by Kishimoto and colleagues, demonstrated that epithelial deletion of Wnt5a from the tracheal epithelium using *ShhCre* did not affect tracheal mesenchymal patterning (Kishimoto et al., 2018). Therefore, we focused our studies on mesenchymal deletion of Wnt5a, wherein cartilage develops. Analysis of whole mount images and cross sections of *Dermo1Cre;Wnt5a<sup>fl/fl</sup>* trachea demonstrated the deficiencies in tracheal elongation as early as E11.5 (Figure 1D), and reduced number of cartilaginous rings by E14.5 (Figure 1F), in agreement with published studies (Kishimoto et al., 2018; Li et al., 2005). Strikingly, we detected a larger field of Sox9 positive cells (chondroblasts) in the Wnt5a deficient trachea as early as E11.5 (Figures 1G,H) that is also noticeable at E13.5 (Figures 1I, J). At this developmental stage we observed more defined cartilaginous rings as well as abnormal organization of the trachealis muscle noticeable by E13.5 (Figures 1E, I, J) a feature previously reported by published studies (Kishimoto et al., 2018; Russell et al., 2023). Taken together, Notum can attenuate the non-canonical induced Wnt5a activity *in vitro*. *In vivo*, Wnt5a is required for proper tracheal elongation, cartilaginous ring number, and shape of the tracheal cartilage.

### Precocious mesenchymal condensation in Wnt5a is associated with JNK and Ca<sup>2+</sup> signaling

Our previous studies determined that lack of Notum delays the mesenchymal condensation, resulting in thinner and mis-patterned cartilage (Gerhardt et al., 2018). Since our observations at E13.5 suggest a precocious condensation in the Wnt5a mutant trachea, we performed a serial analysis of the mesenchymal condensation process from E11.5 to E14.5 in Wnt5a and Notum deficient tracheas. At E11.5, when tracheoesophageal separation is completed, Sox9+ cells are distributed in a continuous stripe for all genotypes analyzed. Interestingly, the Wnt5a deficient trachea (*Dermo1Cre; Wnt5a<sup>fl/fl</sup>*) is already shorter than the control and the Sox9+ area is significantly larger than the control (Figure 1G). Similarly, at E12.5, no presence of aggregation of Sox9+ cells are detected, indicating that no mesenchymal condensations are visible (Figures 2A, B); however, as early as E13.0, we noticed the formation of mesenchymal nodules, which become clearly defined by E13.5 in Wnt5a deficient trachea (Figures 2D, N, Q) as opposed to the control wherein mesenchymal

condensations are less compact (Figures 2C, M, Q). By E14.5 both control and Wnt5a deficient tracheas show distinctive Sox9+ cartilaginous rings and a shorter trachea in mutants compared to controls (Figures 2E, F). Contrasting this finding and concordant with our published studies, mesenchymal condensations are delayed until E14.5 in the Notum deficient tracheas (*Notum*<sup>150/150</sup>) compared to controls (*Notum*<sup>300/300</sup>) (Figures 2G–L, O–Q). To further understand the underlying mechanism by which Wnt5a and Notum could affect the timing of the mesenchymal condensation, we performed an air-liquid interface (ALI) culture using trachea-lung tissue isolated from E12.5 *Sox9KieGFP* mice. Tissue treated with ABC99, a Notum inhibitor, shows no sign of cartilaginous mesenchymal condensations at 42 h compared to control (Figure 3A; Supplementary Video S2, compared to control Supplementary Video S1). The treatment recapitulates the *in vivo* findings observed in the Notum deficient trachea (Figures Fig2G–L). Wnt5a has been shown to act via Ror1/2 receptors activating  $\beta$ -catenin independent Wnt signaling pathways (Kishimoto et al., 2018), including planar cell polarity (PCP) and Calcium dependent signaling (Chae and Bothwell, 2018; Kikuchi et al., 2011). Thus, we pharmacologically inhibited both pathways in E12.5 *Sox9KieGFP* trachea-lung tissue. Inhibition of non-canonical Calcium dependent Wnt signaling with KN93 (calmodulin kinase (CamK) inhibitor) or inhibition of the PCP pathway with JNK inhibitor cause earlier condensation at 24 h of incubation compared to controls (Figures 3A, B) (Supplementary Videos S3, S4). These findings recapitulate the *in vivo* observations in the Wnt5a deficient trachea and indicate that the Ca<sup>2+</sup> and the JNK non-canonical Wnt pathways are required for regulation of timely mesenchymal condensation and a possible mechanism downstream of Wnt5a.

## Cell mechanisms mediating cartilaginous condensation are altered in Wnt5a deficient and Notum deficient tracheas

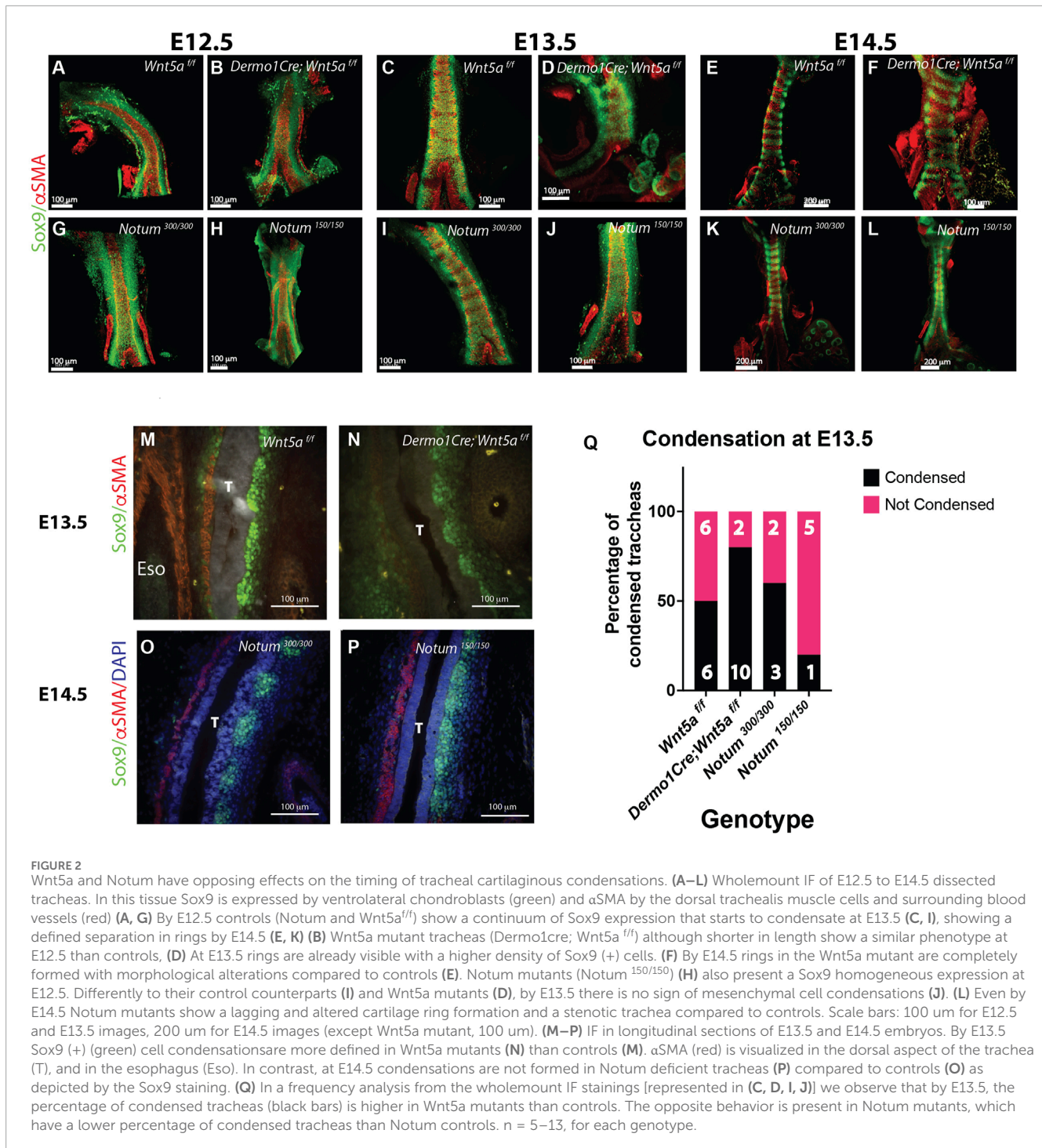
The mesenchymal condensation process requires precise cellular behaviors leading to the compaction of mesenchymal cells (Klumpers et al., 2014). Thus, we sought to investigate whether essential mechanisms mediating mesenchymal cell condensation are affected in Wnt5a and Notum mutants. Evaluation of the migratory ability of E13.5 Wnt5a deficient mesenchymal cells in a wound healing assay revealed that after 24 h, the Wnt5a knockout cells average a 40% closure of the wound area compared to almost 50% for the control; however, no statistical differences are detected. Further, valuation of the wound-healing assay using Notum deficient cells (*Notum*<sup>150/150</sup>) did not show statistically significant differences; however, Notum knockout cells appear moving faster than controls (Figures 4A, B).

Since migration of condensing cells is a local process of directional movement induced by cues present in the mesenchymal ECM, we investigated whether the directional migration toward fibronectin is affected in E13.5 cells of Wnt5a, and Notum deficient tracheal mesenchymal cells in comparison to their respective controls. Notably, the Notum deficient cells had the highest directional migratory ability in this haptotaxis assay, while the Wnt5a mutant cells did not differ from the control (Figure 4C). Compaction of mesenchymal cells requires changes in cell-cell and

cell-substrate adhesion; we tested the adhesion of E13.5 tracheal primary mesenchymal cells as micromasses. When seeded as micro masses, Notum knockout cells show a trend towards reducing cell adhesion compared to controls. Wnt5a knockout cells show a slight increase in cell adhesion compared to controls; however, no significant differences are observed among the genotypes (Figure 4D). Since mesenchymal condensations occur prematurely in Wnt5a deficient tracheas (Figures 2E, F), with cells already condensed by E13.5, we analyzed whether cell-cell adhesion molecules are prematurely expressed in Wnt5a mutant tracheas. Thus, we performed N-cadherin immunofluorescence stainings at E11.5 (Figures 4E–J). N-cadherin is an essential molecule mediating the adhesion of condensed cells. We observed an increased expression of N-cadherin in *Dermo1Cre; Wnt5a<sup>fl/fl</sup>*, at E11.5, finding validated by the quantification of the staining normalized to the Sox9+ cells area (Figure 4K). Further, Sox9 staining depicts Sox9+ cells appearing more compacted as opposed to the loose appearance of the Sox9+ cells in the *Wnt5a<sup>fl/fl</sup>* trachea (Figures 4D, E). Taken together, changes in cellular behavior partially account for the differences in the timing of chondrogenesis in the Wnt5a knockout and Notum knockout tracheas. The increased movement of Notum knockout cells at E13.5 evident in the haptotaxis assay likely explains the delayed chondrogenesis at E14.5, while, the precocious expression of N-cadherin at E11.5 influence the earlier chondrogenesis, in mutant Wnt5a tracheas.

## Molecular signatures in Wnt5a deficient trachea indicate premature activation of a gene expression network leading to a chondrogenic process

Based on changes in cell-cell adhesion and the premature condensation observed in the Wnt5a deficient trachea, we tested the hypothesis that Wnt5a prevents premature mesenchymal condensation via modulation of chondrogenic gene expression. The transition from E11.5 to E13.5 is critical for tracheal development. During these stages a distinct tracheal tube is formed consisting of Nkx2.1+ epithelium surrounded by its unique mesenchyme. By E13.5 trachealis muscle will be organized in the dorsal side, while the mesenchymal condensations that give rise to tracheal cartilage are initiated in the ventral mesenchyme. To define molecular mechanisms explaining the cellular behaviors observed in the Wnt5a deficient trachea, we first performed RNA seq analysis of E11.5 vs E13.5 wild type tracheal tissue to determine changes in gene expression occurring between these critical developmental stages (Figure 5A). Genes differentially regulated and augmented at E13.5 include those encoding ECM molecules *Acan* and *Col9a1*, the transcription factor *Barx1*, and signaling molecules such as *Gdf5*, which is essential for cartilage formation (Figure 5A). Among biological processes enriched at E13.5, those related to skeletal development, ECM organization, and cartilage development were more significant. Top induced pathways include “ECM organization” and signaling pathways, including FGF and TGF-beta signaling pathways (Figure 5B). Next, we performed whole bulk RNA seq on E11.5 tracheas of *Wnt5a<sup>fl/fl</sup>* and *Dermo1Cre; Wnt5a<sup>fl/fl</sup>* mice. We selected this stage because the trachea is fully separated from the esophagus, and it precedes the morphological changes



associated with mesenchymal chondrogenesis. Furthermore, we inferred from our previous findings that *Wnt5a* deficient tracheas may start the chondrogenic process precociously. An unbiased gene expression profiling analysis of *Wnt5a* mutant vs. control shows a premature upregulation of chondrogenic genes by E11.5, including *Col2a1*, a marker of chondrogenesis. We also detected that genes that are normally upregulated at E13.5 in control trachea, i.e., *Gdf5*, *Barx1*, *Col9a1*, are also prematurely induced in the *Wnt5a* mutant, at E11.5, supporting the notion that the chondrogenic program is precocious in the absence of *Wnt5a*

(Figure 5C). In agreement with this finding, biological processes enriched in the mutant *Wnt5a* trachea include those such as cartilage development, chondrocyte differentiation, and regulation of the Wnt signaling pathway (Figure 5D). However, we did not observe changes in Wnt/ $\beta$ -catenin targets *Notum*, *Lef1* and *Axin2* in *Wnt5a* deficient tracheal tissue (Supplementary Figures S2A–D). Since cell compaction induces specific cell differentiation processes in mesenchymal condensations, we examined expression levels of genes encoding transcription factors with a cis-regulatory binding region capable of regulating chondrogenesis. As anticipated,

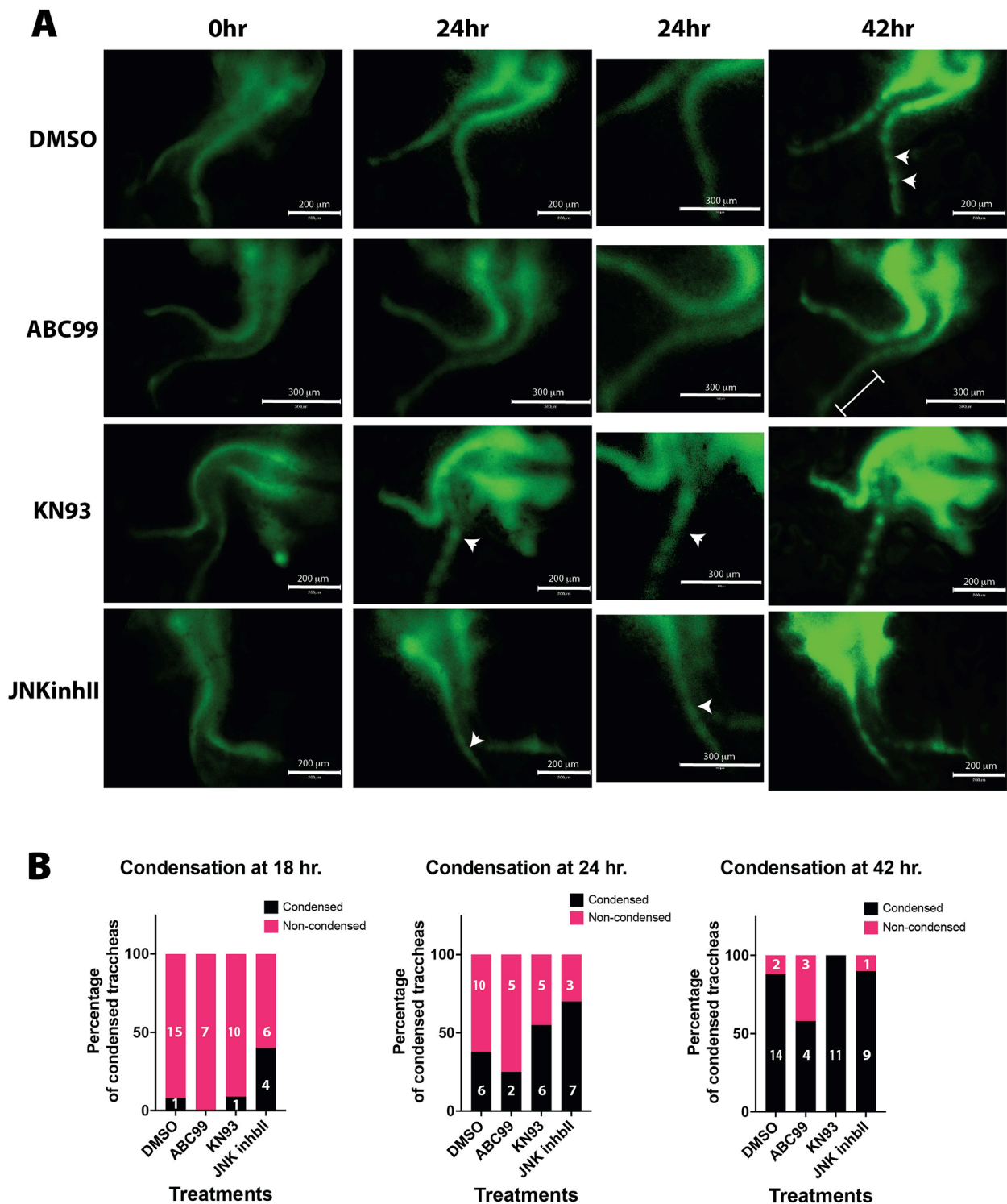


**FIGURE 3**  
 Pharmacological treatments recapitulate Wnt5a-deficient and Notum-deficient phenotypes *ex vivo*. **(A)** Timelapse imaging of larynx-trachea-lung dissected tissue from E12.5 embryos grown *ex vivo* in Air Liquid Interphase (ALI). Endogenous expression of Sox9KleGFP was used to visualize the moment of cell condensation that precedes the formation of cartilage. Condensations in *ex-vivo* explants were defined as SOX9 GFP + cells that formed aggregates and became segmented as time progressed. Vehicle treated tissue (DMSO) shows signs of condensation at 42 h of incubation (white arrows). This phenomenon is absent when Notum is chemically inhibited (ABC99) (white bracket). Inhibitors of the Wnt non-canonical pathway, Calmodulin Kinase inhibitor (KN93) and JNK inhibitor (JNKinhII), induce earlier signs of Sox9KleGFP (+) condensations at 24 h (white arrows), earlier than vehicle treated samples. Scale bar 300  $\mu$ m. Digital zoom for images at 24 h is shown, scale bar 150  $\mu$ m. **(B)** In a frequency analysis from the ALI cultured samples, we observed a trend towards a higher percentage of condensations as early as 18 h in JNKinhII treated samples compared to vehicle treated samples. At 24 h KN93 and JNKinhII show higher percentages of tracheal condensations than vehicle treated samples. ABC99 treated samples show a reduced percentage of tracheal condensations at 18, 24 and 42 h compared to vehicle or other treatments. n = 7–16 for each treatment.

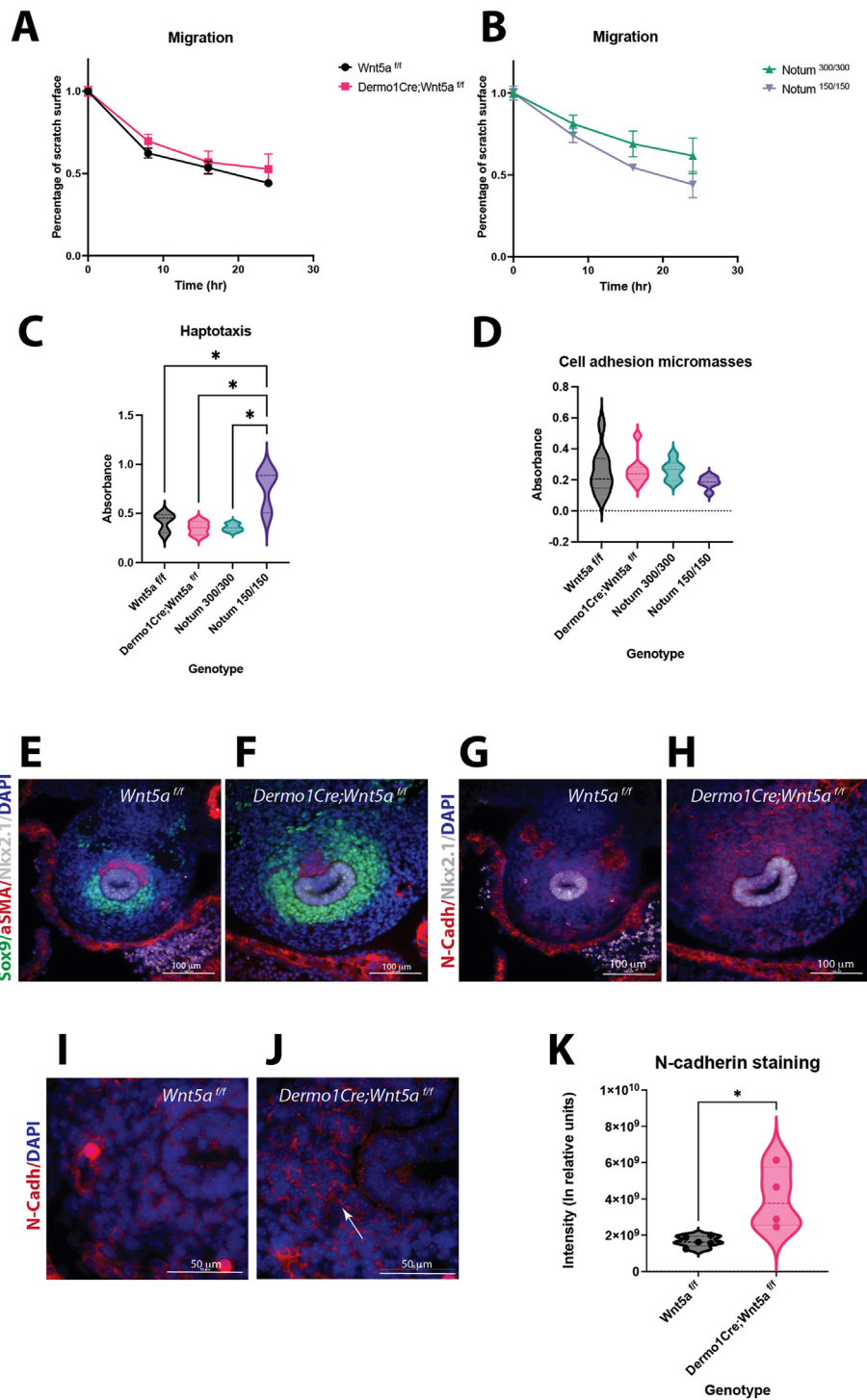


**FIGURE 4** Wnt5a and Notum deletion have unique effects in cell behavior. **(A)** Migration assays of E13.5 primary mesenchymal tracheal cells show no statistical differences in cell motility between *Wnt5a* controls (*Wnt5a<sup>fl/fl</sup>*, black circles) and *Wnt5a* mutants (*Derma1Cre; Wnt5a<sup>fl/fl</sup>*, pink squares). **(B)** There is a trend towards a higher motility of Notum mutants (*Notum<sup>150/150</sup>*, purple triangles) compared to Notum controls (*Notum<sup>300/300</sup>*, green triangles) at 16 and 24 h n = 3 for each genotype. **(C)** Haptotaxis assays of E13.5 primary mesenchymal tracheal cells show an increase in directional cell migration towards fibronectin for Notum mutants (purple) compared to Notum controls (green) and other genotypes. *Wnt5a* mutants (pink) do not show a difference in directional cell migration compared to *Wnt5a* controls (black). n = 3 per genotype. \*p < 0.05 One-way ANOVA. **(D)** Cell adhesion in micromasses from E13.5 primary mesenchymal tracheal cells showed no differences in the genotypes analyzed. n = 6–9 per genotype. **(E–J)** Immunofluorescence stainings of E11.5 cross sections. Sox9 (+) (green) area is larger in *Wnt5a* mutants **(F)** compared to controls **(E)**. N-cadherin (N-cad, red) is increased in *Wnt5a* mutants **(H)** compared to controls **(G)**. Respiratory epithelium identity is maintained (Nkx2.1, white). 40x images. N-cadherin expression is stronger in the cell-cell interphase of dorso-lateral mesenchymal cells in mutants **(J)** compared to controls **(I)**. 100x oil immersion images. DAPI (blue) was used to stain the nuclei. **(K)** N-cadherin intensity quantification normalized to Sox9 + area of the experiments presented in **(E–J)** shows an increase for *Wnt5a* mutants (pink) compared to controls (black). n = 4–5 per genotype, \*p = 0.01 T-test.

transcription factors such as *Barx1*, *Osr2*, *Hoxc5*, and *Tbx18* are differentially regulated in E13.5 wild type tracheas (Figure 5E). Remarkably these genes are also upregulated at E11.5 in the *Dermo1Cre; Wnt5a<sup>ff</sup>* trachea (Figure 5F). The data support a model whereby the expression of *Wnt5a* modulates the timely activation of the chondrogenic process in tracheal mesenchyme by controlling gene expression associated with chondrocyte differentiation.

## Coordinated regulation of the chondrogenic program by Wnt ligands

Our *in vitro* studies demonstrated that Notum modulates *Wnt5a*-induced activity (Figure 1C). On the other hand, deletion of *Wnt5a* accelerates the chondrogenesis program, a phenotype somewhat opposed to the Notum deficient trachea, wherein chondrogenesis is delayed (Figures 2O, P). We reasoned those molecular signatures contributing to the premature condensation observed in the *Dermo1Cre; Wnt5a<sup>ff</sup>* trachea might be downregulated in the Notum model wherein condensation is delayed. To test this concept, we performed gene expression analysis of chondroblast cells of *Notum* deficient tracheas at E13.5, a developmental stage when cartilaginous mesenchymal condensation is already initiated in the wild-type trachea (Figure 6A). Supporting our published studies, the dataset reveals increased expression of Wnt signaling related genes such as *Axin2*, *Ctnnb1*, *Lef1* (Figure 6A). Our RNA seq data identified several genes associated with Wnt/ $\beta$ -catenin independent signaling pathway differentially regulated in Notum deficient tissue, including *Dvl1*. *Dvl1* is an intracellular transducer mediating different non-canonical Wnt pathways (Sharma et al., 2018). Variants in *DVL*, together with variants in *WNT5a* and *ROR2*, have been associated with Robinow syndrome, a condition associated with skeletal malformations (Konopelski Snavely et al., 2023). We also detected upregulation of *Fat1* a gene associated with PCP, encoding an atypical cadherin playing a critical role in directed cell migration and cell-cell contact (Peng et al., 2021) (Figure 6A). Despite these changes in gene expression associated with non-canonical Wnt signaling supporting a potential increase in the pathway activity, we did not observe a significant increased expression of *Wnt5a* in *Notum* deficient tracheas, while levels of *Axin2* are increased [Supplementary Figures S2E–H (Gerhardt et al., 2018)]. Interestingly, genes encoding members of the BAF chromatin remodeling complex, *Arid1a*, *Smarca4*, and *Smarca2* (Alfert et al., 2019) were upregulated after deletion of Notum (Figure 6A). These genes are critical for lineage specification by modulating chromatin accessibility and interacting with transcription factors to affect gene expression and cellular processes (Barnada et al., 2024).

In *Notum* mutant samples, we did observe differential expression of genes mediating mesenchymal cell differentiation, such as *Egf10*, *Bmp3*, *Gata4*, *Col2a1*, and an increased expression of genes influencing cartilage formation including *Sox5*, *Msx2*, and *Arid5a* (Figure 6B). Further, genes involved in cartilage development, condensation, and mesenchymal cell differentiation were largely induced based on the functional enrichment analysis. Corroborating ours and others published findings, pathways enriched included Wnt signaling, Notch, and TGFbeta (Figure 6C). We then compared the differentially regulated genes in response to *Wnt5a* deletion vs

Notum deletion and detected a discrete list of commonly regulated genes after deleting either *Wnt5a* or Notum. For some of these genes, the RNA seq predicted opposite regulation; however, other genes, such as *Col2a1*, were upregulated in both datasets (Figure 6D). A delayed chondrogenic program in the Notum model could partially explain the data. To validate the findings of the RNAseq studies, we performed RNA *in situ* hybridization in samples of E11.5 *Wnt5a<sup>ff</sup>* (control) and *Dermo1Cre; Wnt5a<sup>ff</sup>* (mutant) and E13.5 *Notum<sup>300/300</sup>* (control) and *Notum<sup>150/150</sup>* (mutant) (Figure 6E). We first tested expression of *Gdf5*, which encodes a secreted growth factor promoting cartilage and bone development. As predicted by the analysis of developmental differential gene expression (Figure 5A), levels of expression of *Gdf5* were low at E11.5 as demonstrated by the small number of transcripts detected in *Wnt5a* controls when compared to E13.5 Notum control trachea. On the contrary levels of *Gdf5* transcripts were highly increased in the *Wnt5a* deficient trachea, resembling the E13.5 expression pattern (Figures 5A,C). No differences in expression levels of *Gdf5* are detected in *Notum* control and *Notum* deficient trachea. *Igf1* transcripts, encoding a growth factor necessary for postnatal lung alveologenesis (Gao et al., 2022), were increased in the dorsal and to some degree the ventral mesenchyme of the *Wnt5a* deficient trachea and with a similar expression pattern seen at E13.5 control trachea. No significant differences in *Igf1* expression were observed between control and *Notum* deficient trachea. *Gata4* transcripts, encoding a transcription factor required for muscle development and pulmonary lobar morphology (Ackerman et al., 2007), appear decreased in the distal ventral mesenchyme of *Wnt5a* deficient trachea, and increased in the peripheral ventral mesenchyme of *Notum* deficient trachea. *Osr2* transcripts (Rankin et al., 2012) are observed in an opposite pattern, wherein transcripts are barely detected in *Wnt5a* tissue and slightly increased in the epithelium of the *Wnt5a* deficient trachea, while decreased in the epithelium and ventral distal mesenchyme of the *Notum* deficient trachea (Figure 6E).

Since the RNA seq data suggest that the transcriptional program controlled by *Wnt5a* and Notum are unique to each molecule with limited number of common targets, we tested whether increased levels of *Wnt5a* could account for delayed chondrogenesis as observed in Notum deficient trachea. For this purpose, we performed ALI culture of explants isolated at E12.5 and incubated with *Wnt5a* conditioned media or in presence of the Notum inhibitor ABC99. Trachea lung explants were harvested at 42 h, time when condensations were observed in control tracheal tissue (Figure 3A). After collecting the tissue, explants were processed for whole mount immunofluorescence to determine the expression patterns of Sox9 and  $\alpha$ SMA. As anticipated, in DMSO treated tracheas Sox9 positive cells condensed forming clear bands of cell aggregates. Strikingly, tracheas incubated in presence of *Wnt5a* conditioned media do not condense or condensation was lagging when compared to control DMSO treatment. The finding recapitulates the observed lack of mesenchymal condensation seen after treatment of the trachea-lung explants with ABC99 (Figures 7A, B). The fact that treatment with conditioned *Wnt5a* media caused the delay of mesenchymal condensations made us consider whether in the Notum mutant the delayed mesenchymal condensation is caused by increased levels of *Wnt5a*. To test this possibility, we designed a genetic rescue experiment by generating embryos of genotype *Dermo1Cre; Wnt5a<sup>f/wt</sup>; Notum<sup>150/150</sup>* and we

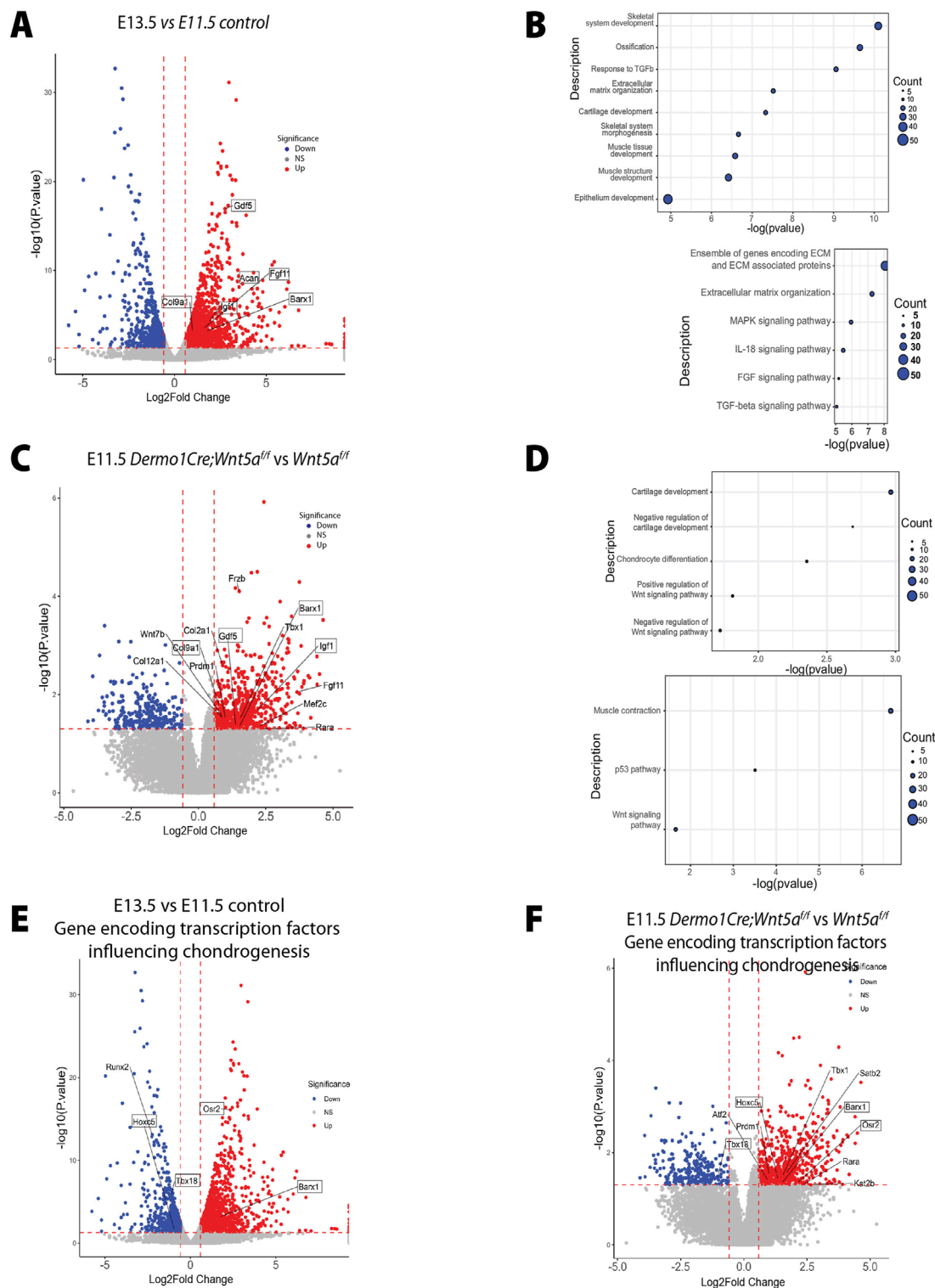
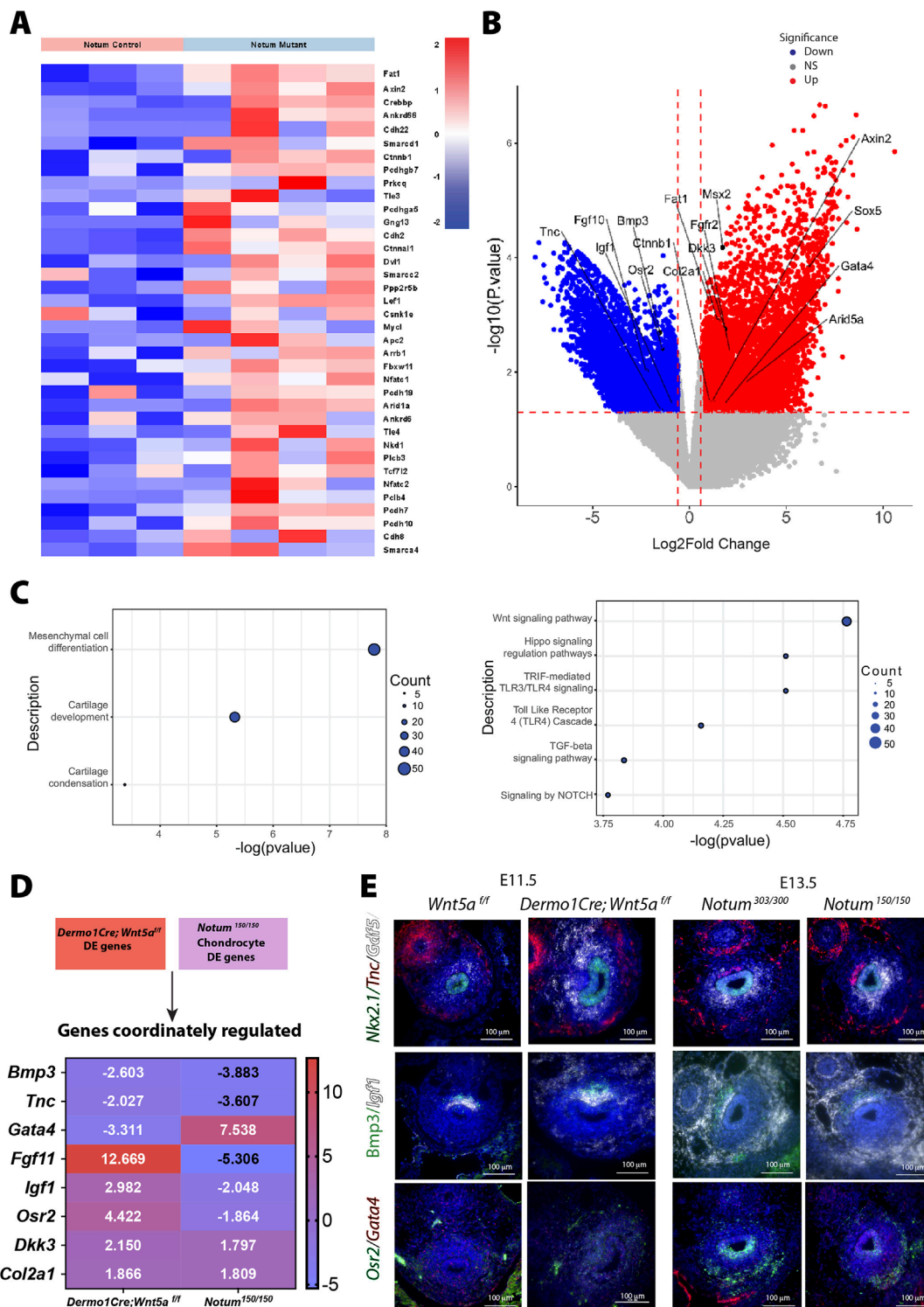


FIGURE 5

The genetic signature associated with cartilaginous tracheal development is prematurely activated in the absence of *Wnt5a*. (A) Volcano plot depicting E13.5 vs. E11.5 genes of interest which have been differentially regulated. Specifically, *Gdf5*, *Col9a1*, *Igf1*, *Barx1*, and *Acan* are upregulated at E13.5. Blue: downregulated, red: upregulated genes. (B) Bubble plots depicting E13.5 vs. E11.5 biological processes and pathway enrichments with significance. (C) Volcano plot depicting E11.5 *Dermo1Cre;Wnt5a<sup>fl/fl</sup>* vs. *Wnt5a<sup>fl/fl</sup>* genes of interest which have been differentially regulated. Specifically, *Gdf5*, *Col9a1*, *Igf1*, and *Barx1* are upregulated at E11.5 after the conditional deletion of *Wnt5a*. Blue: downregulated, red: upregulated genes. (D) Bubble plots depicting E11.5 *Dermo1Cre;Wnt5a<sup>fl/fl</sup>* vs. *Wnt5a<sup>fl/fl</sup>* biological processes and pathway enrichment with significance. (E, F) Volcano plot depicting differentially regulated genes of interest encoding transcription factors capable of binding to cis-regulatory regions of chondrogenic genes of E13.5 vs. E11.5 (E) and E11.5 *Dermo1Cre;Wnt5a<sup>fl/fl</sup>* vs. *Wnt5a<sup>fl/fl</sup>* (F). *Osr2* and *Barx1* are upregulated while *Tbx18* and *Hoxc5* are downregulated in the E13.5 vs. E11.5 dataset. *Tbx18*, *Hoxc5*, *Osr2*, and *Barx1* are upregulated in the E11.5 *Dermo1Cre;Wnt5a<sup>fl/fl</sup>* vs. *Wnt5a<sup>fl/fl</sup>* dataset. Blue: downregulated, red: upregulated genes.



**FIGURE 6**  
Notum differentially regulates Wnt signaling pathway and cartilage development. **(A)** Heat map demonstrates differential expression of Wnt signaling pathway genes among Notum control (Notum<sup>300/300</sup>) and mutant (Notum<sup>150/150</sup>) cells of the tracheal chondroblasts at E13.5. The dataset reveals increased expression of *Axin2*, *Ctneb1*, *Dkk3*, and *Dvl1*. **(B)** Volcano plot depicting genes of interest in Notum mutant (Notum<sup>150/150</sup>) vs. control (Notum<sup>300/300</sup>) which have been differentially regulated in tracheal chondroblasts. Blue: downregulated, red: upregulated genes. NS: non-significant. **(C)** Bubble plots depicting Notum biological processes and pathway enrichments with significance are shown. **(D)** Heatmap of common genes differentially regulated in cells of *Derma1Cre;Wnt5a<sup>fl/fl</sup>* and *Notum<sup>150/150</sup>* chondrocytes. *Gata4* appears more upregulated in Notum cells while *Fgf11* and *Osr2* appear more upregulated in *Derma1Cre;Wnt5a<sup>fl/fl</sup>* cells. Blue: downregulated, red: upregulated genes. **(E)** RNA *in situ* hybridization depicts localization of transcripts for *Nkx2.1*, *Tnc*, *Gdf5*, *Bmp3*, *Igf1*, *Osr2*, and *Gata4* in transverse sections of E11.5 *Wnt5a<sup>fl/fl</sup>*, *Derma1Cre;Wnt5a<sup>fl/fl</sup>*, E13.5 *Notum<sup>303/300</sup>*, and *Notum<sup>150/150</sup>* tracheas. *Osr2* appears to be more abundant at E13.5 in control tracheas and to some degree in *Wnt5a* mutant tracheas. *Gdf5* appears more abundant in E11.5 *Wnt5a* mutant tracheas and in E13.5 controls which validates previous RNAseq findings.

evaluated the presence of mesenchymal condensations at E13.75 in whole mount immunofluorescence (Figure 7C). The Sox9 staining revealed that condensations were visible in the control embryos ( $Wnt5a^{f/wt}; Notum^{300/150}$ ,  $Dermo1Cre; Wnt5a^{f/wt}; Notum^{300/150}$ , or  $Dermo1Cre; Notum^{300/150}$ ) and were not detected in the Notum deficient embryos ( $Wnt5a^{f/wt}; Notum^{150/150}$ ). Strikingly, in embryos of genotype  $Dermo1Cre; Wnt5a^{f/wt}; Notum^{150/150}$ , condensations were visible as determined by the Sox9 staining.

We previously demonstrated that Wnt/ $\beta$ -catenin activity in tracheal mesenchyme is critical for cartilaginous and smooth muscle cell differentiation and patterning (Russell et al., 2023). Since deletion of Notum increases levels of canonical Wnt signaling targets (Supplementary Figure S2) and increased levels of Wnt/ $\beta$ -catenin signaling impair tracheal mesenchymal differentiation (Gerhardt et al., 2018), we also tested whether canonical Wnt signaling could play a role in the delayed chondrogenesis observed in the Notum deficient tracheas. To this purpose, we performed ALI cultures, as previously described, and simultaneously inhibited Wnt/ $\beta$ -catenin and Notum using XAV939 (Huang et al., 2009) and ABC99, respectively. While pharmacological inhibition of Notum caused lack of mesenchymal condensations at 42 h, inhibition of Wnt/ $\beta$ -catenin, did not have a clear effect on timing of mesenchymal condensations. Furthermore, combined treatment of XAV939 and ABC99 did not rescue the lack of mesenchymal condensations at 42 h in ALI culture (Figures 7D, E). Taken together, the data support a model wherein Wnt5a plays a critical role in controlling the timing of the cartilaginous mesenchymal condensation while Notum attenuates Wnt5a activity.

## Conclusion

Our previous studies demonstrated that ablation of Wnt ligand secretion, primarily acting via Wnt/ $\beta$ -catenin signaling, prevents the formation of cartilage giving rise to collapsed and stenotic trachea surrounded by ectopic muscle. In the present study, we demonstrated that Wnt5a-mediated  $\beta$ -catenin independent signaling supports the timely formation and maturation of the cartilaginous tracheal rings. We also determined functional relationships between Notum and Wnt5a, wherein Notum can inactivate canonical and non-canonical Wnt signaling. Wnt5a deficiency leads to an earlier chondrogenesis, while Notum mutants present a delayed chondrogenesis (Figure 7C). Furthermore, increased levels of Wnt5a leads to delayed chondrogenesis recapitulating the phenotype observed after deletion of Notum. Thus, Wnt5a, likely via PCP/JNK and Calcium pathways, is required as a checkpoint to prevent premature mesenchymal condensation, while Notum balances levels of canonical and non-canonical Wnt signaling necessary for the timing of tracheal mesenchymal condensations (Figures 7F–G).

## A role for Notum in the regulation of non-canonical Wnt signaling

A large body of literature has focused on the role of Notum as a regulator of Wnt/ $\beta$ -catenin signaling in *in vitro* studies and different animal models (Kakugawa et al., 2015; Madan et al., 2016;

Zhang et al., 2015). Our previous studies have demonstrated a critical role for Notum in regulating canonical Wnt signaling *in vitro* and *in vivo* during tracheal development (Gerhardt et al., 2018). Furthermore, since Notum can modulate Wnt/ $\beta$ -catenin, inhibition of Notum might be putative therapeutics for diseases characterized by increased Wnt/ $\beta$ -catenin signaling. As an extracellular molecule, Notum constitutes an excellent druggable target (Bayle et al., 2021).

While it has been demonstrated that Notum downregulates Wnt/ $\beta$ -catenin signaling, less is known of its effect in non-canonical Wnt signaling. Studies in liver fibrosis indicate that *in vitro*, Notum reduced the Wnt5a-induced pJNK activity in hepatic cells (Li et al., 2019). Our investigations have demonstrated that *in vitro* Notum prevents the non-canonical response induced by Wnt5a. Our *ex-vivo* studies support a model whereby increased, Wnt5a-induced-signaling, leads to the activation of  $\beta$ -catenin independent pathways mediated by PCP/JNK and Calcium resulting in a delayed chondrogenic process recapitulating the observed phenotype in the Notum deficient trachea. Thus, it is likely that augmented Wnt5a activity partially accounts for the delayed mesenchymal process in Notum deficient tracheas.

## Wnt5a and Notum influence chondrogenic programs

At the molecular level, we have identified differentially regulated genes when comparing the tracheal prechondrogenic mesenchyme at E11.5 and the chondrogenic mesenchyme at E13.5. Notably, these genes mediate processes related to ECM organization, pathways encoding ECM and ECM-related genes, and cartilage formation. We also determined that several of these ECM-related and chondrogenic genes were precociously expressed at E11.5 in Wnt5a mutants or downregulated at E13.5 after the deletion of Notum such as *Osr2*. Besides its role in early respiratory tract specification (Rankin et al., 2012), recent studies have demonstrated a role for *Osr2* integrating biomechanical signaling sensing the stiffness and ECM changes characteristic of tumors (Zhang et al., 2024). The constituents of the ECM support cell aggregation in chondrogenic nodules by coordinating the availability and diffusion of signals and inhibitors (Ono et al., 2009) and restrains cells in a compressed form to sustain differentiation induced by the physical compression (Mammoto et al., 2015). The ECM also facilitates the intracellular communication necessary for condensations by supporting gap junctions between cells and reducing the extracellular space between cells thus, increasing the tissue density (Fowler and Larsson, 2020). Simultaneously, changes in ECM composition will affect the fluidity of the mesenchyme promoting patterning (Huycke et al., 2023; Palmquist et al., 2022). Recent studies have shown that Vangl and Wnt5a are required for the fluidity of the pulmonary mesenchyme during sacculcation (Paramore et al., 2024). In the present study, we detected that N-cadherin expression is increased at E11.5 in the prechondrogenic mesenchyme of the Wnt5a mutants. The augmented expression of N-cadherin has been associated with active mesenchymal condensation before overt chondrogenic differentiation, and N-cadherin expression is essential for mesenchymal condensation mediating both cell-cell interactions and formation of intracellular adhesion complex (Delise

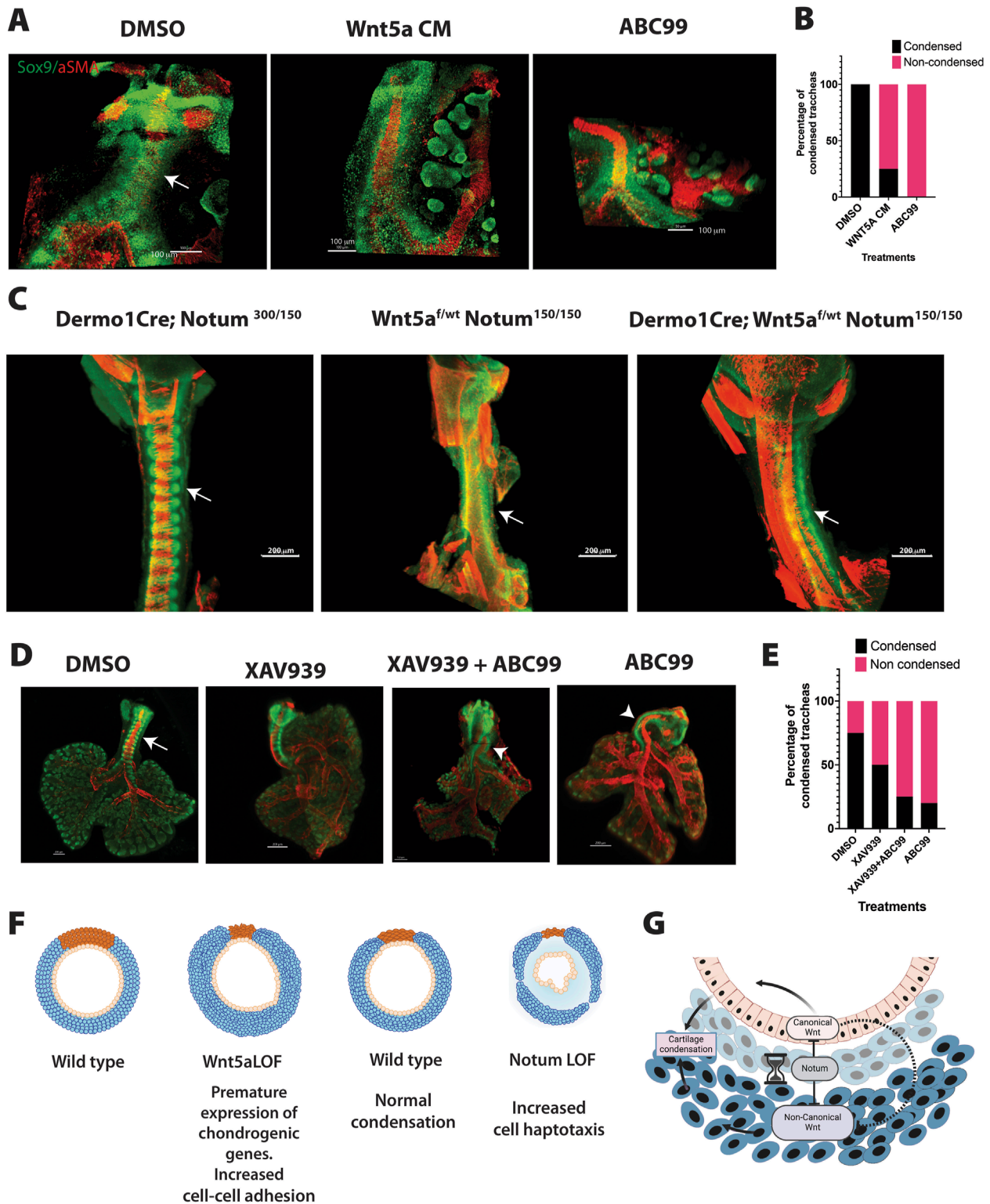


**FIGURE 7** Integration of Wnt5a and Notum activity influence tracheal cartilaginous ring patterning. **(A)** Whole mount immunofluorescence imaging of wild type tracheal lung explants are depicted after 42 h after ALI cultures. Sox9 (green) is expressed in chondroblasts and epithelial cells of the distal lung.  $\alpha$ SMA (red) is localized in muscle cells of the dorsal trachea and bronchi. In vehicle treated tracheas, condensations were clearly observed at 42 h (arrow DMSO). In contrast, addition of Wnt5a conditioned media in media culture prevented the formation of cartilaginous mesenchymal condensations, recapitulating the phenotype obtained after treatment with ABC99, a Notum inhibitor. **(B)** Frequency analysis depicting the effects of the treatments based on the whole mount images represented in **(A)**. N = 4–8 per treatment. **(C)** Whole mount immunofluorescence of E13.75 embryos of a Notum Wnt5a allelic series demonstrating the rescue of the timing of mesenchymal condensations by decreasing the Wnt5a expression in Notum deficient background (*Dermo1Cre; Wnt5a<sup>f/wt</sup>; Notum<sup>150/150</sup>*) as demonstrated by the Sox9 staining (green). Images are representative of embryos from three (Continued)

## FIGURE 7 (Continued)

different litters. (D) Whole mount immunofluorescence imaging of wild type tracheal lung explants are depicted after 42 h after in ALI cultures. In vehicle treated tracheas, condensations were clearly observed at 42 h (arrow DMSO). While addition of ABC99 prevented the formation of cartilaginous mesenchymal condensations, combined addition of XAV939 with ABC99 did not have effect in rescuing the lack of mesenchymal condensations (arrowhead). (E) Frequency analysis depicting the effects of the treatments based on the whole mount images represented in (D). N = 4–5 per treatment. (F) The cartoon summarizes the effects of deletions of Wnt5a and Notum in mesenchymal cell condensation and cartilage. Deletion of Wnt5a (Wnt5a LOF) causes premature condensation of chondroblasts associated with increased cell-cell addition and the premature expression of genes promoting mesenchymal condensations at E11.5. On the other hand, after deletion of Notum (Notum LOF), mesenchymal condensations are delayed in association with increased cell directional migration at E13.5. In both models, the normal morphology of the cartilage is disrupted. (G) Proposed model integrating Notum, Wnt5a and Wnt/ $\beta$ -catenin signaling based on findings from this work and previously published studies. Notum balances Wnt signaling in developing trachea by directly inhibiting the activity of both Wnt5a-mediated signaling and Wnt/ $\beta$ -catenin signaling. Indirectly, by modulating activity of canonical Wnt signaling, Notum may also influence canonical Wnt signaling competition with non-canonical Wnt signaling. Created with [BioRender.com](https://www.biorender.com).

and Tuan, 2002; Wang et al., 2020). Thus, the increased levels of N-cadherin at E11.5 in Wnt5a deficient trachea further support the concept of Wnt5a as a gatekeeper of the timing of mesenchymal condensations via modulating the expression of N-cadherin, ECM, and chondrogenic related genes.

It has been proposed that Wnt/ $\beta$ -catenin dependent and independent signaling can influence each other (Bryja et al., 2009). Whether increased levels of  $\beta$ -catenin mediated signaling play a role in the anomalous condensation observed in Wnt5a deficient tracheas would require further analysis. Our data, based on the expression of canonical targets of Wnt/ $\beta$ -catenin: *Lef1*, *Axin2*, and *Notum* (Supplementary Figures S2A–D) does not support this statement.

Our studies demonstrate that Notum, attenuates levels of canonical and non-canonical Wnt signaling to balance the activity of both branches of the pathway [Figure 1C and (Gerhardt et al., 2018)]. In fact, analysis of the gene expression, indicates differential regulation of Wnt signaling after deletion of Notum in the developing trachea, including both Wnt/ $\beta$  catenin dependent and independent targets (Figure 6A). This supports the role of Notum in attenuating both signaling pathways at the transcriptional level, which ultimately will contribute to the proper patterning and timing of the mesenchymal condensations.

## Timing of the condensation and effects on cartilage patterning and shape

After deletion of Wnt5a, the shape and number of cartilages are altered; each ring appears ticker than in the wild type, but the number of rings is reduced. The reduced number of rings might result from geometrical constraints due to the faulty axial elongation observed after the deletion of Wnt5a (Kishimoto et al., 2018; Onesto et al., 2019). Conversely, the shape and timing of the mesenchymal condensation may impact chondrogenesis and the shape of the final cartilage. Studies in zebrafish have demonstrated that the position and longevity of the mesenchymal condensation affect the size and shape of facial cartilages in zebrafish (Paudel et al., 2022). In this model, the interplay of the Fgf and Notch signal is essential to determine the shape of the cartilaginous condensation. In chicken and mouse embryos, Shh mediating signaling is required for proper tracheal ring orientation (Kingsley et al., 2023). Thus, an early condensation may prevent cells from being exposed to

signals triggered either by the epithelium or other mesenchymal cells within the trachea or the adjacent heart that will determine each cartilaginous ring's final shape and size.

On the contrary, Notum is characterized by cartilaginous rings thinner than the wild type, with a mild reduction in the number of cartilaginous rings (Gerhardt et al., 2018). In this model, we demonstrated that mesenchymal condensation is delayed, a phenotype that in the present work is recapitulated *ex vivo* when control tracheas were treated with Wnt5a conditioned medium (Figure 7A). Furthermore, *in vivo*, reduction of Wnt5a partially rescues the delayed mesenchymal condensation in Notum deficient trachea. Thus, the timing of the mesenchymal condensation has an impact on the shape of the cartilage by altering the exposure of cells to signals required for differentiation and maturation of mesenchymal cells into cartilage.

Finally, it should be taken into consideration the likely heterogeneity of the Sox9 positive cells in the tracheal mesenchyme. The heterogeneity of the cells may affect their response to Wnt5a and Notum signaling during the condensation process; however, this analysis is beyond the scope of this study and will be addressed in a follow up manuscript using single cell sequencing.

## Future directions

While we have demonstrated that mesenchymal Wnt5a partially delays tracheal chondrogenesis, at least in part, by influencing the expression of chondrogenic genes via activation of Camk and JNK, and that an excess of Wnt5a leads to delayed mesenchymal condensation, questions about the molecular mechanism remain unanswered. Specifically, what signaling pathway(s) is/are repressed by Wnt5a to ensure the timely expression of genes required for condensation and cartilaginous differentiation? Is Notum working as a timekeeper by balancing Wnt ligand levels (both canonical and non-canonical) enabling the timely formation of cartilaginous condensations? Do Wnt5a and Notum functionally interact to influence ECM-encoding gene expression to affect the fluidity of the tissue and, thus, the timing of mesenchymal condensations? Will the timing of mesenchymal condensation impact other cell lineages, including the dorsal-ventral patterning and differentiation of the tracheal epithelium? Future studies are guaranteed to answer these questions.

## Data availability statement

The datasets presented in this study can be found in online repositories. The names of the repository/repositories and accession number(s) can be found below: <https://www.ncbi.nlm.nih.gov/geo/>, GSE260707, GSE241175.

## Ethics statement

The animal study was approved by IACUC- Cincinnati Children's Hospital Medical Center- Research Foundation. The study was conducted in accordance with the local legislation and institutional requirements.

## Author contributions

NB-A: Conceptualization, Data curation, Formal Analysis, Investigation, Methodology, Validation, Visualization, Writing—original draft, Writing—review and editing. MM: Data curation, Investigation, Methodology, Validation, Visualization, Writing—review and editing. ST: Investigation, Methodology, Validation, Visualization, Writing—review and editing. KB: Data curation, Formal Analysis, Investigation, Methodology, Writing—review and editing. NR: Data curation, Formal Analysis, Investigation, Visualization, Writing—review and editing. YW: Data curation, Formal Analysis, Investigation, Visualization, Writing—review and editing. YX: Data curation, Formal Analysis, Investigation, Methodology, Visualization, Writing—review and editing. DS: Conceptualization, Formal Analysis, Funding acquisition, Investigation, Methodology, Project administration, Supervision, Validation, Writing—original draft, Writing—review and editing.

## Funding

The author(s) declare that financial support was received for the research and/or publication of this article. This work was partially supported by NIH-NHLBI R01 144774 and HL156860 to DS.

## References

- Ackerman, K. G., Wang, J., Luo, L., Fujiwara, Y., Orkin, S. H., and Beier, D. R. (2007). Gata4 is necessary for normal pulmonary lobar development. *Am. J. Respir. Cell Mol. Biol.* 36, 391–397. doi:10.1165/rcmb.2006-0211RC
- Alfert, A., Moreno, N., and Kerl, K. (2019). The BAF complex in development and disease. *Epigenetics Chromatin* 12, 19. doi:10.1186/s13072-019-0264-y
- Anders, S., and Huber, W. (2010). Differential expression analysis for sequence count data. *Geno. Biolo.* 11(10), R106. doi:10.1186/gb-2010-11-10-r106
- Baarsma, H. A., Königshoff, M., and Gosens, R. (2013). The WNT signaling pathway from ligand secretion to gene transcription: molecular mechanisms and pharmacological targets. *Pharmacol. Ther.* 138, 66–83. doi:10.1016/j.pharmthera.2013.01.002
- Barna, M., and Niswander, L. (2007). Visualization of cartilage formation: insight into cellular properties of skeletal progenitors and chondrodysplasia syndromes. *Dev. cell* 12, 931–941. doi:10.1016/j.devcel.2007.04.016
- Barnada, S. M., Giner de Gracia, A., Morenilla-Palao, C., López-Cascales, M. T., Scopa, C., Waltrich, F. J., et al. (2024). ARID1A-BAF coordinates ZIC2

## Acknowledgments

We appreciate the comments on the manuscript and the project by Dr. Whitsett and Dr. Chen. The authors would like to thank Chuck Crimmel for assistance with graphic design and Joe Kitzmiller for assistance with video processing.

## Conflict of interest

The authors declare that the research was conducted in the absence of any commercial or financial relationships that could be construed as a potential conflict of interest.

## Generative AI statement

The author(s) declare that no Generative AI was used in the creation of this manuscript.

## Publisher's note

All claims expressed in this article are solely those of the authors and do not necessarily represent those of their affiliated organizations, or those of the publisher, the editors and the reviewers. Any product that may be evaluated in this article, or claim that may be made by its manufacturer, is not guaranteed or endorsed by the publisher.

## Supplementary material

The Supplementary Material for this article can be found online at: <https://www.frontiersin.org/articles/10.3389/fcell.2025.1523833/full#supplementary-material>

genomic occupancy for epithelial-to-mesenchymal transition in cranial neural crest specification. *Am. J. Hum. Genet.* 111, 2232–2252. doi:10.1016/j.ajhg.2024.07.022

Bayle, E. D., Svensson, F., Atkinson, B. N., Steadman, D., Willis, N. J., Woodward, H. L., et al. (2021). Carboxylesterase Notum is a druggable target to modulate wnt signaling. *J. Med. Chem.* 64, 4289–4311. doi:10.1021/acs.jmedchem.0c01974

Bottasso-Arias, N., Leesman, L., Burra, K., Snowball, J., Shah, R., Mohanakrishnan, M., et al. (2022). BMP4 and Wnt signaling interact to promote mouse tracheal mesenchyme morphogenesis. *Am. J. Physiol. Lung Cell Mol. Physiol.* 322, L224–L242. doi:10.1152/ajplung.00255.2021

Brownfield, D. G., de Arce, A. D., Ghelfi, E., Gillich, A., Desai, T. J., and Krasnow, M. A. (2022). Alveolar cell fate selection and lifelong maintenance of AT2 cells by FGF signaling. *Nat. Commun.* 13, 7137. doi:10.1038/s41467-022-34059-1

Bryja, V., Andersson, E. R., Schambony, A., Esner, M., Bryjova, L., Biris, K. K., et al. (2009). The extracellular domain of Lrp5/6 inhibits noncanonical Wnt signaling *in vivo*. *Mol. Biol. Cell* 20, 924–936. doi:10.1091/mbc.e08-07-0711

- Caldeira, I., Fernandes-Silva, H., Machado-Costa, D., Correia-Pinto, J., and Moura, R. S. (2021). Developmental pathways underlying lung development and congenital lung disorders. *Cells* 10 10, 2987. doi:10.3390/cells10112987
- Chae, W. J., and Bothwell, A. L. M. (2018). Canonical and non-canonical wnt signaling in immune cells. *Trends Immunol.* 39, 830–847. doi:10.1016/j.it.2018.08.006
- Chan, H. Y., V, S., Xing, X., Kraus, P., Yap, S. P., Ng, P., et al. (2011). Comparison of IRES and F2A-based locus-specific multicistronic expression in stable mouse lines. *PLoS One* 6, e28885. doi:10.1371/journal.pone.0028885
- Cui, L., Yin, S., Deng, C. L., Li, Y. L., Yang, G. H., Chen, F. G., et al. (2005). Cartilage-derived morphogenetic protein 1 initiates chondrogenic differentiation of human dermal fibroblasts *in vitro*. *Zhonghua Yi Xue Za Zhi* 85, 2331–2337.
- Delise, A. M., and Tuan, R. S. (2002). Analysis of N-cadherin function in limb mesenchymal chondrogenesis *in vitro*. *Dev. Dyn.* 225, 195–204. doi:10.1002/dvdy.10151
- Fowler, D. A., and Larsson, H. C. E. (2020). The tissues and regulatory pattern of limb chondrogenesis. *Dev. Biol.* 463, 124–134. doi:10.1016/j.ydbio.2020.04.009
- Gao, F., Li, C., Smith, S. M., Peinado, N., Kohbodi, G., Tran, E., et al. (2022). Decoding the IGF1 signaling gene regulatory network behind alveologenesis from a mouse model of bronchopulmonary dysplasia. *Elife* 11, e77522. doi:10.7554/eLife.77522
- Gerhardt, B., Leesman, L., Burra, K., Snowball, J., Rosenzweig, R., Guzman, N., et al. (2018). Notum attenuates Wnt/ $\beta$ -catenin signaling to promote tracheal cartilage patterning. *Dev. Biol.* 436, 14–27. doi:10.1016/j.ydbio.2018.02.002
- Goldring, M. B., Tsuchimochi, K., and Ijiri, K. (2006). The control of chondrogenesis. *J. Cell Biochem.* 97, 33–44. doi:10.1002/jcb.20652
- Huang, S. M., Mishina, Y. M., Liu, S., Cheung, A., Stegmeier, F., Michaud, G. A., et al. (2009). Tankyrase inhibition stabilizes axin and antagonizes Wnt signalling. *Nature* 461, 614–620. doi:10.1038/nature08356
- Huycke, T. R., Miyazaki, H., Häkkinen, T. J., Srivastava, V., Barriet, E., McGinnis, C. S., et al. (2023). Patterning and folding of intestinal villi by active mesenchymal dewetting. *Cell* 187(12), 3072–3089.e20.
- Hyatt, B. A., Shangguan, X., and Shannon, J. M. (2002). BMP4 modulates fibroblast growth factor-mediated induction of proximal and distal lung differentiation in mouse embryonic tracheal epithelium in mesenchyme-free culture. *Dev. Dyn.* 225, 153–165. doi:10.1002/dvdy.10145
- Kakugawa, S., Langton, P. F., Zebisch, M., Howell, S. A., Chang, T. H., Liu, Y., et al. (2015). Notum deacylates Wnt proteins to suppress signalling activity. *Nature* 519, 187–192. doi:10.1038/nature14259
- Kikuchi, A., Yamamoto, H., Sato, A., and Matsumoto, S. (2011). New insights into the mechanism of Wnt signaling pathway activation. *Int. Rev. Cell Mol. Biol.* 291, 21–71. doi:10.1016/B978-0-12-386035-4.00002-1
- Kingsley, E. P., Mishkind, D., Hiscock, T. W., and Tabin, C. J. (2023). A dynamic Hedgehog gradient orients tracheal cartilage rings. Cold Spring Harbor laboratory.
- Kishimoto, K., Tamura, M., Nishita, M., Minami, Y., Yamaoka, A., Abe, T., et al. (2018). Synchronized mesenchymal cell polarization and differentiation shape the formation of the murine trachea and esophagus. *Nat. Commun.* 9, 2816. doi:10.1038/s41467-018-05189-2
- Klumpers, D. D., Mao, A. S., Smit, T. H., and Mooney, D. J. (2014). Linear patterning of mesenchymal condensations is modulated by geometric constraints. *J. R. Soc. Interface* 11, 20140215. doi:10.1098/rsif.2014.0215
- Knudson, C. B., and Toole, B. P. (1985). Changes in the pericellular matrix during differentiation of limb bud mesoderm. *Dev. Biol.* 112, 308–318. doi:10.1016/0012-1606(85)90401-4
- Konopelski Snavelly, S. E., Srinivasan, S., Dreyer, C. A., Tan, J., Carraway, K. L., and Ho, H. H. (2023). Non-canonical WNT5A-ROR signaling: new perspectives on an ancient developmental pathway. *Curr. Top. Dev. Biol.* 153, 195–227. doi:10.1016/bs.ctdb.2023.01.009
- Kulyk, W. M., Upholt, W. B., and Kosher, R. A. (1989). Fibronectin gene expression during limb cartilage differentiation. *Development* 106, 449–455. doi:10.1242/dev.106.3.449
- Lawrence, D. P., Gannibal, P. B., and Lawrence, C. B. (2013). The sections of *Alternaria*: formalizing species-group concepts. *Mycologia*. 105(6), 1306–1314. doi:10.3852/13-180
- Li, C., Hu, L., Xiao, J., Chen, H., Li, J. T., Bellusci, S., et al. (2005). Wnt5a regulates Shh and Fgf10 signaling during lung development. *Dev. Biol.* 287, 86–97. doi:10.1016/j.ydbio.2005.08.035
- Li, C., Smith, S. M., Peinado, N., Gao, F., Li, W., Lee, M. K., et al. (2020). WNT5a-ROR signaling is essential for alveologenesis. *Cells* 9 9, 384. doi:10.3390/cells9020384
- Li, W., Yu, X., Zhu, C., Wang, Z., Zhao, Z., Li, Y., et al. (2019). Notum attenuates HBV-related liver fibrosis through inhibiting Wnt 5a mediated non-canonical pathways. *Biol. Res.* 52, 10. doi:10.1186/s40659-019-0217-8
- Madan, B., Ke, Z., Lei, Z. D., Oliver, F. A., Oshima, M., Lee, M. A., et al. (2016). NOTUM is a potential pharmacodynamic biomarker of Wnt pathway inhibition. *Oncotarget* 7, 12386–12392. doi:10.18632/oncotarget.7157
- Mammoto, T., Mammoto, A., Jiang, A., Jiang, E., Hashmi, B., and Ingber, D. E. (2015). Mesenchymal condensation-dependent accumulation of collagen VI stabilizes organ-specific cell fates during embryonic tooth formation. *Dev. Dyn.* 244, 713–723. doi:10.1002/dvdy.24264
- Mammoto, T., Mammoto, A., Torisawa, Y. S., Tat, T., Gibbs, A., Derda, R., et al. (2011). Mechanochemical control of mesenchymal condensation and embryonic tooth organ formation. *Dev. Cell* 21, 758–769. doi:10.1016/j.devcel.2011.07.006
- Mauck, R. L., Seyhan, S. L., Ateshian, G. A., and Hung, C. T. (2002). Influence of seeding density and dynamic deformational loading on the developing structure/function relationships of chondrocyte-seeded agarose hydrogels. *Ann. Biomed. Eng.* 30, 1046–1056. doi:10.1114/1.1512676
- Nasr, T., Holderbaum, A. M., Chaturvedi, P., Agarwal, K., Kinney, J. L., Daniels, K., et al. (2020). Disruption of a hedgehog-foxf1-rspo2 signaling axis leads to tracheomalacia and a loss of sox9+ tracheal chondrocytes. *Dis. Model Mech.* 14, dmm046573. doi:10.1242/dmm.046573
- Nishita, M., Itsukushima, S., Nomachi, A., Endo, M., Wang, Z., Inaba, D., et al. (2010). Ror2/Frizzled complex mediates Wnt5a-induced AP-1 activation by regulating Dishevelled polymerization. *Mol. Cell Biol.* 30, 3610–3619. doi:10.1128/MCB.00177-10
- Ohkawara, B., and Niehrs, C. (2011). An ATF2-based luciferase reporter to monitor non-canonical Wnt signaling in *Xenopus* embryos. *Dev. Dyn.* 240, 188–194. doi:10.1002/dvdy.22500
- Onesto, V., Barrell, W. B., Okesola, M., Amato, F., Gentile, F., Liu, K. J., et al. (2019). A quantitative approach for determining the role of geometrical constraints when shaping mesenchymal condensations. *Biomed. Microdevices* 21, 44. doi:10.1007/s10544-019-0390-0
- Oster, G. F., Murray, J. D., and Maini, P. K. (1985). A model for chondrogenic condensations in the developing limb: the role of extracellular matrix and cell tractions. *J. Embryol. Exp. Morphol.* 89, 93–112. doi:10.1242/dev.89.1.93
- Palmquist, K. H., Tiemann, S. F., Ezzeddine, F. L., Yang, S., Pfeifer, C. R., Erzberger, A., et al. (2022). Reciprocal cell-ECM dynamics generate supracellular fluidity underlying spontaneous follicle patterning. *Cell* 185, 1960–1973.e11. doi:10.1016/j.cell.2022.04.023
- Paramore, S. V., Trenado-Yuste, C., Sharan, R., Nelson, C. M., and Devenport, D. (2024). Vangl-dependent mesenchymal thinning shapes the distal lung during murine sacculation. *Dev. Cell* 59, 1302–1316.e5. doi:10.1016/j.devcel.2024.03.010
- Paudel, S., Gjorcheska, S., Bump, P., and Barske, L. (2022). Patterning of cartilaginous condensations in the developing facial skeleton. *Dev. Biol.* 486, 44–55. doi:10.1016/j.ydbio.2022.03.010
- Peng, Z., Gong, Y., and Liang, X. (2021). Role of FAT1 in health and disease. *Oncol. Lett.* 21, 398. doi:10.3892/ol.2021.12659
- Rankin, S. A., Gallas, A. L., Neto, A., Gomez-Skarmeta, J. L., and Zorn, A. M. (2012). Suppression of Bmp4 signaling by the zinc-finger repressors Osr1 and Osr2 is required for Wnt/ $\beta$ -catenin-mediated lung specification in *Xenopus*. *Development* 139, 3010–3020. doi:10.1242/dev.078220
- Russell, N. X., Burra, K., Shah, R. M., Bottasso-Arias, N., Mohanakrishnan, M., Snowball, J., et al. (2023). Wnt signaling regulates ion channel expression to promote smooth muscle and cartilage formation in developing mouse trachea. *Am. J. Physiol. Lung Cell Mol. Physiol.* 325, L788–L802. doi:10.1152/ajplung.00024.2023
- Ryu, Y. K., Collins, S. E., Ho, H. Y., Zhao, H., and Kuruvilla, R. (2013). An autocrine Wnt5a-Ror signaling loop mediates sympathetic target innervation. *Dev. Biol.* 377, 79–89. doi:10.1016/j.ydbio.2013.02.013
- Shannon, J. M., and Hyatt, B. A. (2004). Epithelial-mesenchymal interactions in the developing lung. *Annu. Rev. Physiol.* 66, 625–645. doi:10.1146/annurev.physiol.66.032102.135749
- Sharma, M., Castro-Piedras, I., Simmons, G. E., and Pruitt, K. (2018). Dishevelled: a masterful conductor of complex Wnt signals. *Cell Signal* 47, 52–64. doi:10.1016/j.cellsig.2018.03.004
- Sinner, D. I., Carey, B., Zgherea, D., Kaufman, K. M., Leesman, L., Wood, R. E., et al. (2019). Complete tracheal ring deformity. A translational genomics approach to pathogenesis. *Am. J. Respir. Crit. Care Med.* 200, 1267–1281. doi:10.1164/rccm.201809-1626OC
- Snowball, J., Ambalavanan, M., Whitsett, J., and Sinner, D. (2015a). Endodermal Wnt signaling is required for tracheal cartilage formation. *Dev. Biol.* 405, 56–70. doi:10.1016/j.ydbio.2015.06.009
- Sucre, J. M. S., Vickers, K. C., Benjamin, J. T., Plosa, E. J., Jetter, C. S., Cutrone, A., et al. (2020). Hyperoxia injury in the developing lung is mediated by mesenchymal expression of Wnt5A. *Am. J. Respir. Crit. Care Med.* 201, 1249–1262. doi:10.1164/rccm.201908-1513OC
- Trapnell, C., Pachter, L., and Salzberg, S. L. (2009). TopHat: discovering splice junctions with RNA-Seq. *Bioinformatics* 25(9), 1105–1111. doi:10.1093/bioinformatics/btp120
- Tada, M., and Heisenberg, C. P. (2012). Convergent extension: using collective cell migration and cell intercalation to shape embryos. *Development* 139, 3897–3904. doi:10.1242/dev.073007
- Voloshanenko, O., Schwartz, U., Kranz, D., Rauscher, B., Linnebacher, M., Augustin, I., et al. (2018).  $\beta$ -catenin-independent regulation of Wnt target genes by Ror2 and ATF2/ATF4 in colon cancer cells. *Sci. Rep.* 8, 3178. doi:10.1038/s41598-018-20641-5

- Wallkamm, V., Dorlich, R., Rahm, K., Klessing, T., Nienhaus, G. U., Wedlich, D., et al. (2014). Live imaging of Xwnt5A-ROR2 complexes. *PLoS One* 9, e109428. doi:10.1371/journal.pone.0109428
- Wang, F., Flanagan, J., Su, N., Wang, L. C., Bui, S., Nielson, A., et al. (2012). RNAscope: a novel *in situ* RNA analysis platform for formalin-fixed, paraffin-embedded tissues. *J. Mol. Diagn* 14, 22–29. doi:10.1016/j.jmoldx.2011.08.002
- Wang, Y., Xiao, Y., Long, S., Fan, Y., and Zhang, X. (2020). Role of N-cadherin in a niche-mimicking microenvironment for chondrogenesis of mesenchymal stem cells *in vitro*. *ACS Biomater. Sci. Eng.* 6, 3491–3501. doi:10.1021/acsbmaterials.0c00149
- Wang, Z., Shu, W., Lu, M. M., and Morrisey, E. E. (2005). Wnt7b activates canonical signaling in epithelial and vascular smooth muscle cells through interactions with Fzd1, Fzd10, and LRP5. *Mol. Cell. Biol.* 25, 5022–5030. doi:10.1128/MCB.25.12.5022-5030.2005
- Widelitz, R. B., Jiang, T. X., Murray, B. A., and Chuong, C. M. (1993). Adhesion molecules in skeletogenesis: II. Neural cell adhesion molecules mediate precartilaginous mesenchymal condensations and enhance chondrogenesis. *J. Cell Physiol.* 156, 399–411. doi:10.1002/jcp.1041560224
- Yadav, U. S., Biswas, T., Singh, P. N., Gupta, P., Chakraborty, S., Delgado, I., et al. (2023). Molecular mechanism of synovial joint site specification and induction in developing vertebrate limbs. *Development* 150, dev201335. doi:10.1242/dev.201335
- Zhang, J., Li, J., Hou, Y., Lin, Y., Zhao, H., Shi, Y., et al. (2024). Osr2 functions as a biomechanical checkpoint to aggravate CD8. *Cell* 187(13), 3409–3426.e24. doi:10.1016/j.cell.2024.04.023
- Zhang, K., Yao, E., Chuang, E., Chen, B., Chuang, E. Y., Volk, R. F., et al. (2022). Wnt5a-Vangl1/2 signaling regulates the position and direction of lung branching through the cytoskeleton and focal adhesions. *PLoS Biol.* 20, e3001759. doi:10.1371/journal.pbio.3001759
- Zhang, X., Cheong, S. M., Amado, N. G., Reis, A. H., MacDonald, B. T., Zebisch, M., et al. (2015). Notum is required for neural and head induction via Wnt deacylation, oxidation, and inactivation. *Dev. Cell* 32, 719–730. doi:10.1016/j.devcel.2015.02.014
- Zhou, Y., Yang, Y., Guo, L., Qian, J., Ge, J., Sinner, D., et al. (2022). Airway basal cells show regionally distinct potential to undergo metaplastic differentiation. *Elife* 11, e80083. doi:10.7554/eLife.80083